PRESSURE DEPENDENCE OF THERMAL CONDUCTIVITY AND INTERFACIAL THERMAL RESISTANCE IN EPOXY SYSTEMS

by

Dedeepya Valluripally

A Thesis

Submitted to the Faculty of Purdue University

In Partial Fulfillment of the Requirements for the degree of

Master of Science in Mechanical Engineering

School of Mechanical Engineering

West Lafayette, Indiana

December 2018

THE PURDUE UNIVERSITY GRADUATE SCHOOL

STATEMENT OF COMMITTEE APPROVAL

Dr. Xiulin Ruan, Chair

School of Mechanical Engineering

Dr. Amy Marconnet

School of Mechanical Engineering

Dr. Liang Pan

School of Mechanical Engineering

Approved by:

Dr. Jay P. Gore

Head of the Graduate Program

ACKNOWLEDGMENTS

Firstly, I would like to express my sincere gratitude and thanks to my advisor, Dr. Xiulin Ruan, the chair of the thesis committee for the continuous support, encouragement and guidance during this research. I'm fortunate to have Dr. Amy Marconnet and Dr. Liang Pan as my committee members. I'm very thankful for their encouragement and insightful comments.

I would like to thank Dr. Vikas Varshney of Air Force Research Laboratory (AFRL) for providing inputs at initial stage and useful discussions and advices throughout the research.

I thank all my fellow research group members, especially, Jihang Zou, Prabudhya Roychowdary and Jingjing Shi for the helpful discussions and suggestions.

Finally, I would like to express my deepest gratitude to my family: my parents, grandparents, my brother and a close friend, Ravichandra Mikkilineni, for all the love, support and continuous encouragement even from thousands of miles away.

TABLE OF CONTENTS

LIST OF TABLES

LIST OF FIGURES

ABSTRACT

Author: Valluripally, Dedeepya. MS
Institution: Purdue University
Degree Received: December 2018
Title: Pressure Dependence of Thermal Conductivity and Interfacial Thermal Resistance in Epoxy Systems
Committee Chair: Xiulin Ruan

Thermal management in electronic devices is one of the biggest challenges faced by the semiconductor industry. Thermal Interface Materials (TIMs) are used in electronics to fill air gaps between the surfaces of integrated circuit (IC) chips to dissipate heat. Polymer-graphene composites, a very promising choice as TIMs also have a drawback of high interfacial thermal resistance and a low thermal conductivity of polymer. It is known from the theoretical models that application of pressure may affect the thermal conductivity in a desirable manner, but quantitative simulations were not available. In this paper, the pressure dependence of thermal conductivity of epoxy and interfacial resistance at epoxy-graphene interface is studied using non-equilibrium molecular dynamics (NEMD) simulations. The results show that the thermal conductivity of epoxy increases with increase in pressure, and they compare well with the predictions using a theoretical model. The interfacial thermal resistance at epoxy-graphene interface reduces with increase in pressure. The reduction is sharp in the beginning and slowly reaches saturation as pressure increases. At 10 GPa compressive pressure, a 90-95% decrease in interfacial thermal resistance is observed.

1. INTRODUCTION AND BACKGROUND

1.1 Introduction

Thermal management of electronic devices is one of the biggest challenges faced by the semiconductor industry. There is an ever-growing quest for miniaturization of devices and need for faster and improved performance. The size of electronic devices has drastically reduced reaching incredible performance levels. There has also been a great improvement in semiconductor technology, diodes, and transistors. Also, there is a growing interest for emerging technologies like flexible/wearable electronics, thermoelectrics etc. However, these advancements have given rise to serious concern of effectively handling the heat dissipation from these devices [1]. Failing to provide effective thermal management will result in high temperatures of the devices thereby affecting the performance and effectiveness. Materials with improved thermal conductivity are needed to achieve this along with effective design of components. Same is the situation in case of Integrated Circuit (IC) chips. The power density of IC chips has been growing considerably over the period of time thereby creating a need for better heat dissipation. Therefore, it is clearly understood that the need for development of novel materials with enhanced thermal conductivities is higher than ever.

Polymers are materials widely used for many applications in adhesives, coatings, integrated memory chips and diodes due to their desirable properties like flexibility, low weight, good electrical resistivity, resistance to many solvents, corrosion resistance, chemical stability and low cost. Polymer based composites are used as Thermal Interface Materials (TIMs) which are materials used to fill the air gap between the contacting surfaces of the IC chip and the heat sink

[2]. The main purpose of TIMs is to enable effective heat dissipation from the surface of the IC chips. But the polymers possess a very low thermal conductivity and are generally induced with materials of high thermal conductivity to improve their heat transfer ability. Hence, TIMs are made of polymer-based material matrix induced with thermally conductive fillers [3].

Epoxy resins are one of the polymer materials extensively used for all applications due to the advantages mentioned above and their mechanical properties and specific strength. However, the thermal conductivity of epoxy resin is as low as 0.2 W m^{-1} K^{-1} as reported by many researchers [4, 5] and also verified in this study. Therefore, epoxy used as the polymer matrix is induced with thermally conductive fillers for TIMs.

Generally, high conductivity materials like copper, silver, aluminum/boron nitride, alumina, graphite and silicon nitride are used as filler materials [2, 6]. In applications requiring an electrical insulation along with high thermal conductivity, electrically insulating materials are used for fillers [6]. The thermal conductivity of TIMs currently used in the industry is in the range of 1 – 10 W m^{-1} K^{-1} [7]. If the thermal conductivity of the TIMs could be further increased successfully, it would be a great step forward for the electronic industry. Recently, significant efforts are being invested in this area to investigate the applicability and performance of several highly conductive materials like graphene and Carbon Nanotubes (CNTs) as fillers [3, 7, 8].

Nanocomposites are composites induced with nanofillers and have a high surface to volume ratio. They have better thermal, electrical and mechanical properties in comparison to the conventional composites. In recent years, a good amount of research is happening on investigating the properties

of carbon nanotubes as nanofiller with epoxy resin [9, 10, 11]. It is observed that introducing CNTs has improved the thermal and mechanical properties of the epoxy composite [12]. However, the CNTs are very expensive materials which limits the scope of application of the CNT based polymer nanocomposites. This problem is solved by the development of economical process for fabrication of graphene [13].

It is well known that graphene exhibits an extremely high thermal conductivity, in fact in a range of 2000 – 3000 W m^{-1} K^{-1} [14, 15] at room temperatures. The introduction of highly conductive graphene fillers into a polymer matrix is a promising solution to improve the thermal conductivity of polymer matrices and in turn the TIMs thus providing enhanced heat dissipation. The thermal conductivity of the polymer nanocomposites is dependent on the thermal conductivity of polymer as well as the filler. Since the thermal conductivity of polymer is very low and acts as the bottleneck of thermal transport, it is especially beneficial to find ways to enhance its thermal conductivity.

Furthermore, in polymer nanocomposites dispersed with graphene, the interaction at the interface between the polymer and graphene has an immense influence on the resultant overall composite properties. Owing to the huge distinction in their thermal properties, the polymer-graphene composites experiences a jump in temperature at the interfaces. The behavior is quantified as the interfacial thermal resistance (ITR) also called as the Kapitza resistance [16]. The thermal conductivity of the polymer-graphene composites is heavily affected by the interfacial thermal resistance and hence ITR plays a crucial role in improving the thermal efficiency of TIMs. Same is applicable in case of epoxy-graphene composites, the focus of interest in this study. Hence, in

the current work, efforts have been made to study the behavior of thermal conductivity of epoxy and the interfacial thermal resistance at the epoxy – graphene interface, both of which are important for better performance of TIMs.

There is rise in need to understand the behavior of thermal properties of polymers and polymer composites at elevated pressures. Experimental data available for thermal conductivity of polymers, epoxy in particular [17, 18], is mostly near atmospheric pressure or at low pressures due to practical limitations. There is still a need for knowledge of behavior of thermal conductivity of epoxy at higher pressures, which is now more feasible with the advance of computer simulations. Interfacial thermal resistance, the other important parameter in performance of composites is also known to depend on pressure [19]. In general, this is also explained by the acoustic mismatch model [20] according to which the interfacial thermal resistance varies proportionally with the acoustic impedance, defined by $(c\rho)^{-1}$, where c is the phonon speed and ρ is the fluid density. Since the density increases as pressure in the system increases, it is expected that the interfacial thermal resistance decreases with increase in pressure. However, there are a few studies [19, 21, 22] on the pressure dependence of interfacial thermal resistance with almost no studies on the same in epoxy-graphene composites. Therefore, a study of kapitza resistance; the behavior of decrease in the resistance with increase in pressure can provide a useful technique to improve efficiency of TIMs and heat dissipation in the devices using them.

Two of the very well-known methods to study the interfacial phonon transmission behaviors are the acoustic mismatch model and the diffusive mismatch model [23]. However, these two models assume a perfectly contacted and strong bonded interface which is clearly not the case in epoxy –

graphene composites. Apart from these, there are means to understand atomic level details using methods like lattice dynamics [24, 25] and molecular dynamics [26] to investigate the behavior of interfacial thermal resistance. Molecular Dynamics (MD) simulation methods, which are based on many body interatomic potentials are very popular and widely used for the analysis of properties at an atomic scale [27]. This is because, they provide a scope to examine and understand even very complex structures at atomic level and evaluate the process at every time step of the simulation.

Therefore, in the current study, the pressure dependent behavior of thermal conductivity in epoxy and interfacial thermal resistance in epoxy – graphene composite systems has been investigated using molecular dynamics simulations.

1.2 Previous Studies

Epoxy has been a subject of interest for the researches since long because of its use in wide range of applications such as adhesives, coatings, composite matrices, integrated circuit chips, semiconductors, diodes and very recently in flexible/wearable and printed electronics such as epoxy ink. Thermal conductivity of epoxy is one of the important properties of interest for reasons discussed in the previous section, however more studies in literature are focused on the mechanical and structural properties. Thermal conductivity of an epoxy resin was initially estimated by D.E. Kline [4] along with few other polymers in the year 1961 and estimated the thermal conductivity to be approximately 0.23 W m^{-1} K^{-1} at near room temperature. In the most recent times, Varshney et al. [5] evaluated the thermal conductivity of cross-linked epoxy resin, EPON-862 with a cross-linking agent DETDA using molecular dynamics simulations. They have performed MD simulations by both EMD and NEMD methods and estimated the value to be in the range of 0.2 - 0.3 W m^{-1} K^{-1}. They have discussed various contributions of heat flux vector to the thermal

conductivity of epoxy. Kumar et al. [28] has performed MD simulations of cross-linked epoxy by EMD approach incorporating a long-range correction technique to reduce the error in measurement of thermal conductivity to within 10% from experimental value. The value of thermal conductivity from the simulations was nearly 0.25 W m^{-1} K^{-1} which matches perfectly with the experimental value. They have also studied the effect of temperature on the thermal conductivity. Early this year, Li et al. [29] has published an interesting study on thermal conductivity of epoxy resin made by parallel linking method. The epoxy designed by this approach has demonstrated an enhanced thermal conductivity of 0.80 W m^{-1} K^{-1} which was further improved drastically by applying a tensile strain in the uniaxial direction along the chain. This study strengthens the idea that application of strain/pressure can yield beneficial results to help in improving the thermal conductivity of epoxies useful for different applications.

The literature is extremely limited on pressure dependence of pure epoxy resins though some published works are available in case of epoxy composites. Andersson et al. [17] first studied the pressure dependence of thermal conductivity of an epoxy resin in 1973, using experimental methods for pressures ranging from 5 to 30 kbar. They have observed an improvement in the thermal conductivity with increase in pressure and that the thermal conductivity dependence on pressure is unaffected by the amount of hardener. Sundqvist et al. [18] studied the thermal conductivity of epoxy up to pressure of 2.5 GPa along with the behavior at two different temperatures 300 and 400 K. However, all such available experimental studies do not venture into high pressure range probably due to the practical limitations in the experimentation methods.

As discussed in the previous section, the advantage of studying the interfacial thermal resistance in polymer-based composites is well understood and therefore a good amount of research has been happening in this interest. Swartz et al. [23] have discussed the interfacial thermal resistance in the very early days of emerging interest and studied the difference in behavior of boundary resistance in two different types of interfaces, gas – solid and solid-solid interfaces by employing the acoustic mismatch model and diffusive mismatch model. Liu et al. [7] have provided an extensive and a very useful summary of different TIMs available including epoxy-based composites along with their interfacial thermal resistance data for different compositions measured mostly by experimental methods. The thermal conductivity for the epoxy composites was in the range of 0.25 – 13 W m^{-1} K^{-1} depending upon the type and concentration of the filler material used. The thermal conductivity was observed to be highest in case of boron nitride, alumina and silicon carbide fillers and on the lower side with the use of diamond, graphite and carbon nanotube fillers due to high interfacial resistance.

An extensive research has been conducted on epoxy – CNT nanocomposites which prove to be very efficient TIMs. Efforts are being made to reduce the interfacial resistance by different methods like functionalization, alignment and surface modification of CNTs. PB Kaul et al. [30] have designed vertically aligned CNTs used in EPON – 862 and studied its thermal properties. The alignment of CNTs has improved the thermal conductivity to 5.28 W m^{-1} K^{-1}. They also demonstrate a chance of reaching values as high as 25 W m^{-1} K^{-1} with proper methods of alignment and fabrication. Sarvar et al. [8] have reviewed most of the available epoxy-based composites in their work and concluded the same about CNTs being effective filler materials if well-aligned. However, the vertical alignment of CNTs from one surface forcing to establish contact with the

opposite surface leads to good conductivity and low thermal resistance with the aligned surface but results in opposite situation on the opposite surface. Along with this, the high cost of CNTs is another challenge limiting the scope of applications. Therefore, the focus has shifted on to graphene fillers which are a cheaper alternative and resolve the alignment issues.

Stankovich et al. [13] provided the fabrication methods to develop graphene-based composites. They used a bottom-up chemical method to fine tune the graphene to improve their performance as filler in a graphene – polystyrene composite. Luo and Lloyd [31] have studied the interfacial thermal transport at graphene – paraffin wax interfaces by non-equilibrium (NEMD) simulations. The reported value of interfacial thermal resistance is in the range of (61.0 ± 4.7) MW m^{-2} K^{-1}. This work is a good reference for the modelling method and MD simulations of polymer-graphene interfaces. They have also studied the size effect on the boundary transport in graphene- paraffin systems which is a commonly observed phenomenon in NEMD simulations. Along the same lines, Wang et al. [32] have performed NEMD simulations on epoxy-graphene systems, the subject of interest in this current work. The interfacial thermal resistance at epoxy – graphene interface was observed to be $(0.713 \pm 0.036) \times 10^{-8}$ W m^{-2} K^{-1}. They have also studied the effect of functionalization of graphene on the boundary resistance and show results that functionalization reduces the interfacial thermal resistance at epoxy – graphene interface.

Researchers have investigated different types of functionalization methods to improve the interface properties of graphene fillers [2, 33]. Another useful alternative to improve interfacial thermal properties is applying a strain/pressure on the interface as discussed in section 1.1. There are few studies in literature looking at the pressure dependent behavior of interfacial thermal resistance.

Pressure dependence studies have been conducted at gold/water and silicon/water interfaces [19], metallic silicon and Si (Ge) and aluminum-silicon interfaces [34]. Liu et al. [35] studied the tensile and compressive strain effects in graphene – silicene interfaces showing that the thermal conductance at interface decreased by almost 47% at 7% tensile strain loading in the interface direction. Similarly, at graphene-MoS_2 interface, Ding et al. [36] observed a 70% decrease and a 150% increase in interfacial thermal conductance at 5% tensile and 5 % compressive strain application. C Liu et al. [22] studied the effect of pressure on interfacial thermal resistance of few-layer graphene by using non-equilibrium Green function (NEGF) method. They have demonstrated nearly 4 times decrease in the interfacial thermal resistance at a 10 GPa pressure by compression.

However, there weren't any studies found in the literature on pressure dependence of interfacial thermal resistance at epoxy – graphene interfaces by any method.

1.3 Objectives

Based on the importance and need for study of thermal properties in epoxy and epoxy composites discussed in section 1.1 and the knowledge of previous studies mentioned in section 1.2, the following are the objectives of this current research.

1. Evaluate the thermal conductivity of epoxy by use of molecular dynamics simulations and study the pressure dependence of the thermal conductivity in the range of 0 – 10 GPa.
2. Estimate the interfacial thermal resistance at epoxy-graphene interfaces by performing molecular dynamics simulations and study the pressure dependence of the interfacial thermal resistance in the range of 0 – 10 GPa.

1.4 Thesis Outline

Described in this section is a brief outline of the chapters in this thesis. There are totally 5 chapters in this thesis including Chapter 1, introduction and background.

Chapter 2 provides a brief insight into the fundamentals of molecular dynamics simulations with details of formulation and MD algorithm, several parameters used in the MD simulations and the software used to perform the simulations.

Chapter 3 provides complete details of development of molecular models and force fields, methods used to evaluate the properties and the simulation details.

Chapter 4 includes all the results obtained in a systematic manner along with a discussion. It consists of two sections. The first section is a detailed discussion on evaluation of thermal conductivity of epoxy and the pressure dependence of the thermal conductivity at given pressures. Similarly, second section consists of a discussion on evaluation of interfacial thermal resistance at epoxy-graphene interface and the pressure dependence of the interfacial thermal resistance.

Chapter 5 consists of the concluding remarks and the future scope of work of this thesis.

2. FUNDAMENTALS OF MOLECULAR DYNAMICS

2.1 MD Background

The study of properties at microscopic scales has always been important. Computer simulations are a very useful tool to perform such studies in situations where experimental feasibility is limited due to practical conditions and to complement the results achieved by experimental methods. There are two main types of techniques for atomistic simulations, namely Molecular Dynamics and the Monte Carlo simulations. Though the Molecular Dynamics simulations have been around for quite a while, the widespread use and the ability to build even complex polymer or biological structures [37] has improved due to the advent of high-performance computing. This study adopts the Molecular Dynamics method to study the thermo-physical properties of epoxy and the epoxy-graphene interfaces. Molecular Dynamics is a method in which the realistic behavior of atoms can be mimicked by making use of an energy potential function and applying Newton's laws of motion. There are several free as well as paid software available for performing Molecular Dynamics simulations. In this study, Large-scale Atomic/Molecular Massively Parallel Simulator (LAMMPS) has been used to perform the simulations. LAMMPS is an open source code from Sandia National Laboratories which is freely available for use [38].

2.2 Fundamentals and Formulation

Molecular Dynamics simulations predict the trajectory of motion of the atoms also including the atomic positions and velocities at each time step. The advantage of these simulations is that the future time step is updated based on the calculations of previous time step. The forces at each time

step are calculated by solving the classical Newton's equations of motion [39]. Thus, the primary equations of MD are the basic equations of motion given by Newton's second law, which are

$$m_i \ddot{r}_i = f_i \tag{2.1}$$

where

f_i - the force on the i^{th} atom

m_i – mass of the i^{th} atom

r_i – position of the i^{th} atom and $\ddot{r}_i$ – acceleration of the i^{th} atom,

The force on the atom is also given by the relation

$$f_i = -\frac{dU_i(r)}{dr_i} \tag{2.2}$$

where U_i is the potential energy of the atom *i.*

The equations of motion for the system can be defined by a derivative of position to give velocity and derivative of velocity to obtain acceleration of the particle.

$$\frac{d(r_i)}{dt} = \dot{r}_i \tag{2.3}$$

$$\frac{d(\dot{r}_i)}{dt} = \frac{f_i}{m_i} \tag{2.4}$$

The above mentioned are a set of ordinary differential equations. For a set of N atoms, there would be a set of 3N position and velocity coordinates making it impossible to obtain an analytical solution. However, the above equations can be solved by a numerical solution approach for which, in general, various time integration algorithms are used during the simulation. The algorithms will further be discussed in section 2.4.

2.3 Molecular Interactions

The molecular interactions can be broadly classified into two types, intramolecular interactions which describe the interaction between atoms of same molecule and intermolecular interactions, which is interaction between atoms of different molecules. Intramolecular interactions consist of bonded type of interactions whereas the intermolecular interactions are the non – bonded type of interactions.

The potential energy function can be defined as

$$U(r) = \sum_{bonds} \frac{1}{2} k_{ij}^{b} \left(r_{ij} - r_{eq}\right)^2 + \sum_{Bond\ angles} \frac{1}{2} k_{ijk}^{a} \left(\theta_{ijk} - \theta_{eq}\right)^2 + \sum_{Dihedrals} \frac{1}{2} k_{ijkl}^{d} \left(1 + \cos\left(n\Phi_{ijkl} - \delta\right)\right) + U_{non-bonded} \quad (2.5)$$

where k_{ij}^{b}, k_{ij}^{a}, k_{ijkl}^{d} are bond, angle and dihedral constants,

r_{ij} is the distance between the atoms *i* and *j*,

θ_{ijk} is the angle between the atoms *i, j* and *k*,

Φ_{ijkl} is the dihedral angle,

r_{eq}, θ_{eq} are the equilibrium bond length and the equilibrium angle respectively.

Intramolecular interactions: The first three are the intramolecular terms that define the bonded type of interactions between two, three or four atoms. The first term represents the bond stretching between two atoms usually defined by a simple harmonic function. The second term, also a harmonic function corresponds to the bending angle between two bonds, i.e. three atoms and the third is the torsional term representing the dihedral angle twisting (including true dihedrals and impropers) defined between three bonds or four atom coordinates. Dihedral term should be

specified in cases where there are four or more atoms joined continuously. These terms are very important to control the structure and stability of the molecule.

Finally, some additional terms may be needed to define certain configurations which are not accounted in the specified torsional terms. The sp^2 carbons in the aromatic rings of epoxy molecule experience out of plane motions and thus need an additional term to account for the corresponding energy. These terms are called the improper torsional terms, given by

$$U_{improper} = \sum_{Impropers} \frac{1}{2} k^{i}_{ijkl}\left(1 + \cos\left(n\Phi_{ijkl} - \delta\right)\right) \tag{2.6}$$

Intermolecular interactions: The last term represents the non-bonded interactions between the atoms which can be of two types. The van der Waals interactions between pair of atoms are defined by using the Lennard Jones 6-12 potential,

$$V_{LJ} = 4\varepsilon\left[\left(\frac{\sigma}{r_{ij}}\right)^{12} - \left(\frac{\sigma}{r_{ij}}\right)^{6}\right] = \varepsilon\left[\left(\frac{r_{eq}}{r_{ij}}\right)^{12} - 2\left(\frac{r_{eq}}{r_{ij}}\right)^{6}\right] \tag{2.7}$$

where ε and σ are the energy potential constants,

r_{ij} is the distance of separation between atoms i and j,

r_{eq} is the equilibrium distance between two atoms, i.e. the distance where the potential is minimum.

The first term, $\left(\frac{r_{eq}}{r_{ij}}\right)^{12}$ defines the repulsive forces experienced when atoms of the molecules come very close to each other and their electron clouds overlap. The second half, $-2\left(\frac{r_{eq}}{r_{ij}}\right)^{6}$ is a dispersion term defining the attractive forces experienced due to a weak dispersion. The van der Waals forces after a certain inter-atomic distance called cutoff distance r_c, can be ignored since

the interactions become weak with long distance. Generally, in MD simulations, a cut-off $r_c = 2.5\sigma$ is used [40]. In the current work, a cut-off of 12.0 Å was employed based on the same principle. In presence of electrostatic charges, Coulomb potential is used to account for the interactions

$$V_{coulomb} = k_e \frac{q_i q_j}{r_{ij}} \tag{2.8}$$

where k_e is the coulomb constant given by $k_e = \frac{1}{4\pi\epsilon_0}$,

ϵ_0 is permissivity of free space,

q_i and q_j are the charges of the atoms with a separating distance of r_{ij}.

The electrostatic forces reduce very slowly with distance and hence care must be taken to handle the long-range forces. Therefore, in case of coulombic interactions, the interactions within the cut-off distance are calculated directly in real space and the interactions beyond the cut-off distance are also calculated, but in k-space (also called reciprocal space).

2.4 MD Algorithm

As discussed in section 2.2, it is impossible to obtain an analytical solution to the set of ordinary differential equations of motion, Equations (2.3) and (2.4). A straightforward solution can be obtained by a finite difference approach [27] applying a 'Time -integration scheme' to estimate the atom parameters by updating the atom position, velocity and acceleration at every step based on previous time step as explained below. Taylor's expansion of the position vector is given by

$$r_i(t + \Delta t) = r_i(t) + v_i(t)\Delta t + \frac{1}{2}a_i(t)(\Delta t)^2 + \frac{1}{6}b_i(t)(\Delta t)^3 + O(\Delta t)^4 \tag{2.9}$$

$$r_i(t - \Delta t) = r_i(t) - v_i(t)\Delta t + \frac{1}{2}a_i(t)(\Delta t)^2 - \frac{1}{2}b_i(t)(\Delta t)^3 + O(\Delta t)^4 \tag{2.10}$$

Adding together the Equations (2.9) and (2.10) gives

$$r_i(t+\Delta t) = -r_i(t-\Delta t) + 2r_i(t) + \frac{1}{2}a_i(t)(\Delta t)^2 + O(\Delta t)^4 \tag{2.11}$$

where $v_i(t)$ – velocity of atom i at time t,

$a_i(t)$ – acceleration of atom i at time t,

Δt – time step.

From the above equation, the position of an atom at any time step $(t+\Delta t)$ can be obtained directly based on its position during a previous time step $(t-\Delta t)$. The acceleration $a_i(t)$ can be calculated by combining the Equations (2.1) and (2.2),

$$m_i\ddot{r}_i + \frac{dU_i(r)}{dr_i} = 0 \tag{2.12}$$

The truncation error in the scheme is of the order $(\Delta t)^4$. This method of updating atom is known as the Verlet algorithm [41]. However, the Verlet algorithm has been further modified to overcome certain limitations.

By applying Verlet algorithm, the velocity at time step t cannot be calculated until the position at future timestep $(t+\Delta t)$ is arrived at. Thus, to overcome this limitation, a new half-step algorithm was proposed by Hockney [42] by modifying the Verlet algorithm. This integration method updates the position and velocity at interleaved points in between actual time steps as

$$r_i(t+\Delta t) = r_i(t) + v_i\left(t+\frac{1}{2}\Delta t\right)\Delta t \tag{2.13}$$

$$v_i\left(t+\frac{1}{2}\Delta t\right) = v_i\left(t-\frac{1}{2}\Delta t\right) + a_i(t)\Delta t \tag{2.14}$$

where $a_i(t)$ is again calculated using Equation (2.14) as in Verlet method. This method is called the Leap-frog integration algorithm.

However, with the modified Verlet i.e. Leap-frog method, the position and velocity of atom are not calculated simultaneously at a particular time step. The method compromises the simplicity and ease of the Verlet algorithm making it complicated to obtain the trajectories of atoms at each timestep.

Therefore, to avoid the complexity, the Verlet algorithm was further modified by Swope et al. [43] to develop a half-step velocity algorithm called the Velocity-Verlet algorithm which is widely used. By employing the Velocity-Verlet algorithm, the trajectories of atoms are updated as follows.

$$r_i(t + \Delta t) = r_i(t) + v_i(t)\Delta t + \frac{1}{2}a_i(t)(\Delta t)^2 \tag{2.15}$$

$$v_i(t + \Delta t) = v_i(t) + \frac{a_i(t) + a_i(t + \Delta t)}{2}\Delta t \tag{2.16}$$

2.5 Force Field and Potentials

In MD simulations, a structure is built by defining a molecule as a set of spheres(atoms) connected by springs(bonds). The bond details like stretch, bend and torsion can be described by equations analogous to spring deformation. This set of equations providing information of bonded and non-bonded interactions used to construct a molecular structure is called the force field. The force field describes the variation of bond length, angle, torsion and non-bonded interactions with respect to time.

In this work, a Consistent Valence Force Field (CVFF) was used to describe the interactions in the epoxy system. The interactions between graphene carbon atoms were defined by Adapted Intermolecular Reactive Empirical Bond Order (AIREBO) potential. The interactions between the epoxy and graphene atoms are van der Waals (vdW) interactions described by the Lennard-Jones potential, Equation (2.7).

2.6 Boundary Conditions

Establishing the boundary conditions is important for performing an MD simulation. The boundaries of the system can be periodic or non-periodic boundaries. Periodic Boundary Conditions (PBC) are commonly used for most of the MD simulations. Molecular Dynamics, as discussed, deals with simulation of a finite system to obtain the motion trajectories of particles to evaluate desired properties. However, most of the properties to be evaluated are at bulk level. Periodic Boundary Conditions come to aid by allowing to simulate a small system (unit cell) and apply PBC to mimic an infinite system. The unit cell is surrounded by its periodic images which are its exact replica as shown in Fig. 1.

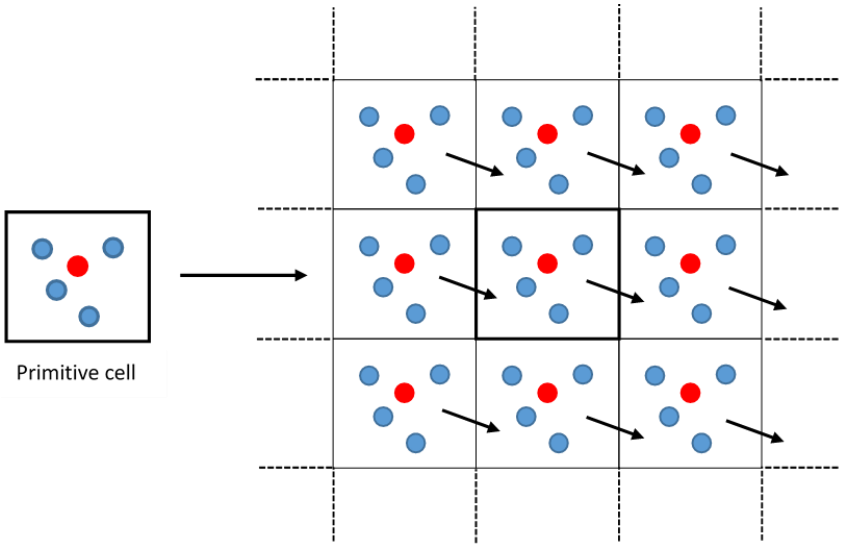

Fig. 1. Two-dimensional schematic of periodic boundary conditions.

Every particle in the surrounding box mimics the trajectories/features of the original particle in the unit cell. If a particle leaves the box in any direction, its periodic image will enter the box from opposite direction. In that way, a homogenous system is generated by eliminating the presence of any free surfaces.

On the other hand, the use of non-periodic boundary conditions doesn't allow any such replication of a system. It deals with simulating a finite system with properties limited to within the system. When interested in calculating non-homogenous properties or interfacial properties, non-periodic boundary conditions may be applied. In this work, periodic boundary conditions have been used to simulate the structure of epoxy, graphene and to evaluate the thermal conductivity.

2.7 Thermodynamic Ensembles

In MD simulations, the properties of a system are calculated by time averaging the values from each time step. Various statistical ensembles are used to perform the averaging. There are manly three popular thermodynamic ensembles used in MD simulations.

NVT (Canonical Ensemble): In this type of thermodynamic ensemble, the N-number of particles, V-volume and T-temperature of the system are conserved. The system exchanges energy with a heat bath to maintain a required temperature and establish a thermal equilibrium. The temperature is a principle variable of a canonical ensemble which can be controlled. Different types of thermostats are available to maintain temperature in the system by adding and removing heat. An NVT ensemble is very useful in cases where a temperature-controlled MD simulation is needed.

NPT (Isobaric-Isothermal Ensemble): It is a statistical ensemble which maintains N-number of atoms, P-pressure and T-temperature of the system constant. It is possible to control both pressure and temperature in this ensemble and hence a thermostat and a barostat are utilized. The volume of the system is not fixed and is allowed to change based on the pressure and temperature. The pressure and volume fluctuations at a particular temperature are related as

$$\beta = -\frac{1}{V}\left(\frac{\partial V}{\partial P}\right)_T = 0 \tag{2.17}$$

where V – volume

P – pressure in the system,

β – isothermal compressibility of the system at temperature T.

NVE (Microcanonical Ensemble): In this thermodynamic ensemble, E-energy is conserved along with N-number of atoms and V-volume instead of pressure and temperature. The system is considered to be isolated with no exchange of energy with environment.

There are also other thermodynamic ensembles like the Grand-Canonical (μVT) ensemble maintained at constant chemical energy, volume and temperature and NPH ensemble with constant number of atoms, pressure and enthalpy. The present work makes use of NVT, NPT and NVE ensembles to perform the MD simulations.

2.8 Temperature and Pressure Controls

There are different methods to control temperature and pressure in MD simulations. The temperature can be controlled by different methods, Anderson, Nosé-Hoover, Berendsen thermostats and Velocity scaling. The thermostat controls the temperature and maintains the system in the correct thermodynamic ensemble. Velocity scaling is a method in which the kinetic

energy of the system is controlled at equilibrium by maintaining the temperature. In case of variation of temperature of outside the range, the atomic velocities rescaled to fall within the range. Pressure control can be performed by various barostats, Berendsen, Parinello, Anderson and Nosé-Hoover. The Nosé and Anderson barostats maintain the desired pressure by allowing the volume of the cell to change but retain the shape of the cell.

In this work, the Nosé-Hoover thermostat and barostat are used during the simulation in NVT and NPT ensembles and the Berendsen thermostat was used in the NVE ensemble to introduce and remove heat from the system to establish a temperature gradient for calculation of interfacial thermal resistance.

2.9 Energy Minimization

Before performing the actual MD simulations, it is important that the system is prepared suitably. Energy minimization is performed on the system in conjunction with MD simulations before or during the process, to modify the atom positions to reach the lowest energy level. In Energy minimization, the atom positions are slightly adjusted by using an iterative method called Conjugate Gradient (CG) method [44]. The method starts with an initial guess value, searching for solution from each iteration and check whether closer to solution. It stores the successive search information and accordingly shape the system to reach a minimum. The process of energy minimization continues till there is no significant change in energy between the last and before-last time-steps. The position of minimum energy of a system is at the lowest point of the well of distance vs. energy plot as shown in Fig. 2. The shape/geometry of the system gets modified in a step by step process until lowest point is reached.

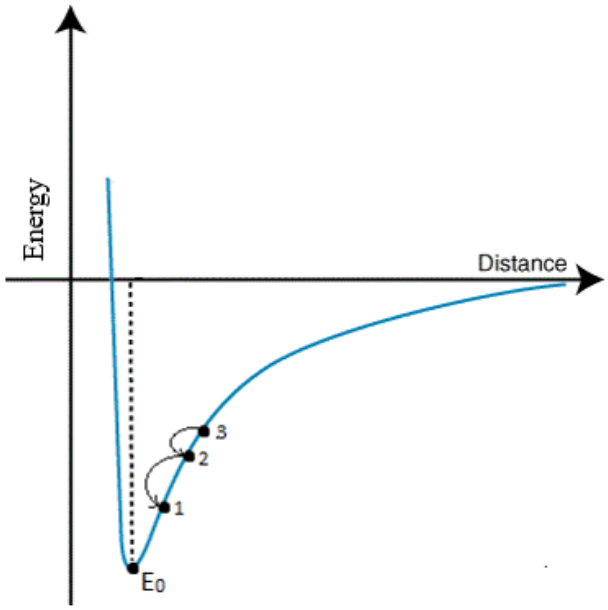

Fig. 2. Energy vs. Distance plot showing minimum energy point.

For systems with large polymers or complex structures, reaching the exact lowest point during the energy minimization might be difficult. The system reaches to a state closest possible to the lowest energy point.

3. MOLECULAR MODELLING AND METHODS

3.1 Structure

3.1.1 Epoxy

The initial structure of uncrosslinked Epoxy resin with curing agent along with the potential parameters was obtained from Vikas Varshney of Air force Laboratory, developed using an atomistic modelling tool and used in their published work [5]. The Epoxy resin structure developed is of EPON 862 (Diglycidyl Ether of Bisphenol F) and the crosslinking agent is DETDA (Diethyltoluenediamine) in 2:1 ratio. EPON 862 is a chemical compound formed by combining an epoxide with Bisphenol - F . Bisphenol – F has different isomer configurations such as ortho-ortho, ortho-para and para-para. Para-para isomers are widely used for epoxy resin formations due to their better melt viscosity and physical properties. A para-para configuration of Bisphenol - F in EPON 862 is shown in the Fig. 3. A curing agent is generally used to harden the resin during applications. DETDA (Diethyltoluenediamine) is used as the curing agent for epoxy resin. The molecular structure of EPON 862 and DETDA molecules is shown in Fig. 3

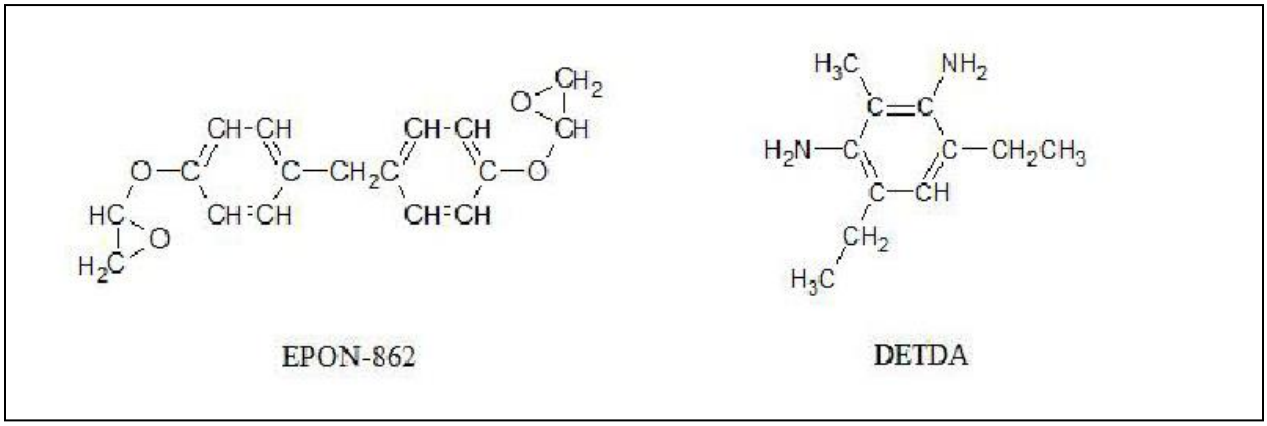

Fig. 3. Molecular structure of EPON-862 and DETDA. Reproduced with permission from reference [45],copyright 2012, John Wiley and Sons.

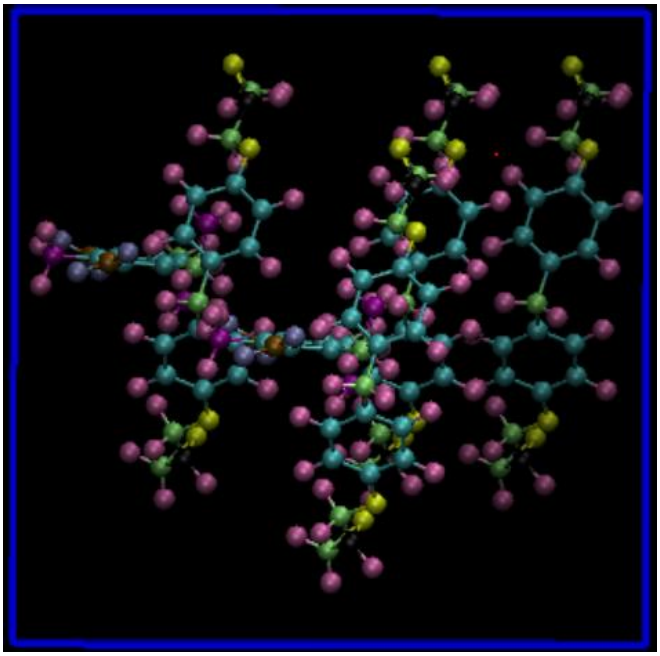

Fig. 4. Initial structure of epoxy containing 4 molecules of Epon-862 and 2 molecules of DETDA.

The initial structure is periodic cell of 21Å x 21 Å x 21 Å with 6 molecules (4 EPON 862, 2 DETDA) and consisting of 234 atoms, generated using periodic boundary conditions. The structure shown in above Fig. 4 consists of 8 atom types. The aromatic carbons have been defined as Type 1. All the aliphatic carbons have been defined of same type except the carbons of ether group in EPON 862 and the CH_2 group attached to the phenyl ring of the DETDA molecule. These carbons have been defined as a different type to facilitate a cross-linking reaction if desired. The Consistent Valence Forcefield (CVFF) has been used for the simulation of the Epoxy molecules and the interactions were defined by Lennard – Jones (LJ) potential. The potential parameters for different atom types were obtained from the software [5]. The details of LJ pair potential coefficients used are mentioned in Table 1.

Table 1. LJ potential parameters for Epoxy and Graphene.

Atom type	Energy constant, ε (eV)	Distance Constant, σ (Å)
Aromatic carbon	0.006418	3.6170487995
Aliphatic carbon	0.001691	3.8754094636
Hydrogen	0.001648	2.4499714540
Nitrogen	0.007242	3.5012320066
Oxygen	0.009887	2.8597848722
Carbon in Graphene	0.002390	3.4120000000

The LJ potential parameters for interactions between different atom types are obtained by using Lorentz-Berthelot mixing rules [46, 47]

$$\varepsilon_{ij} = \sqrt{\varepsilon_{ii}\varepsilon_{jj}} \tag{3.1}$$

$$\sigma_{ij} = \frac{\sigma_{ii} + \sigma_{jj}}{2} \tag{3.2}$$

Where ε_{ij} – energy constant between atom type i and j

σ_{ij} – distance constant between atom type i and j.

The Epoxy structure has 14 bond types, 25 angle types, 31 dihedral and 6 improper types. The initial structure of epoxy containing 6 molecules is first subject to an energy minimization to fine-tune the atom coordinates iteratively so that the system reaches a minimum potential energy level [48]. The obtained model of 21x21x 21 $Å^3$ is then replicated 3 times to 63x63x63 $Å^3$ box with 12:6 molecule ratio. The replicated model is then equilibrated in an NVT ensemble at a temperature of 300 K to achieve a reasonable velocity distribution. Energy minimizations have been performed from time to time in between the steps to minimize the system's energy to a stable level. The resulting structure is then subjected to an NPT simulation to achieve the desired density of 1.2 g/cc

[49]. NVT and NPT ensembles make use of the Nośe-Hoover's thermostat and barostat settings for the simulation. The size of the box has been reduced to approximately 40x40x40Å^3 during the NPT simulation. The resulting final structure was used as the structure of epoxy for further molecular dynamics simulations to study properties like thermal conductivity, bulk modulus and interfacial resistance at epoxy-graphene interface as described in the next sections.

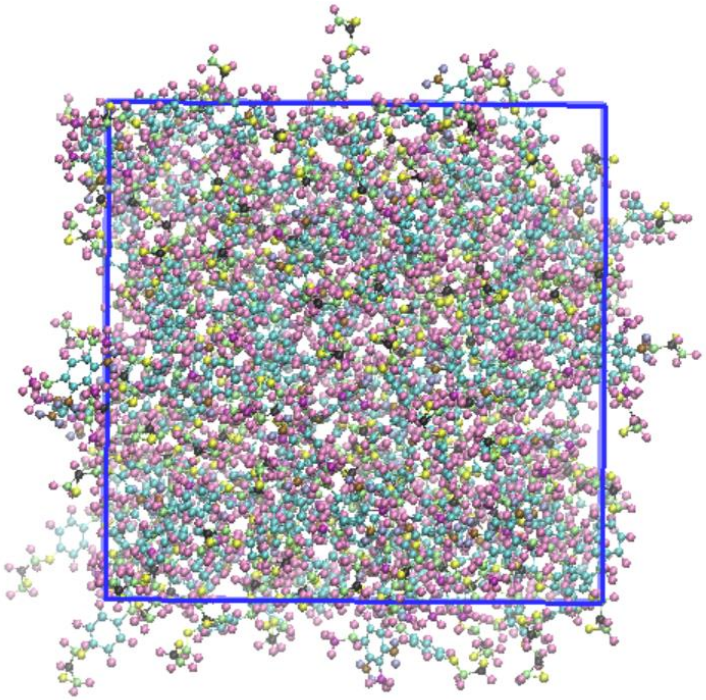

Fig. 5. Final Structure of epoxy after equilibration.

To estimate the thermal conductivity of epoxy and to study the pressure dependence of thermal conductivity, the structure was replicated 3 times in the Z – direction to obtain a longer domain (with Z dimension greater than cross-section) which is desirable in Non- Equilibrium Molecular Dynamics (NEMD), the chosen approach for estimation of thermal conductivity.

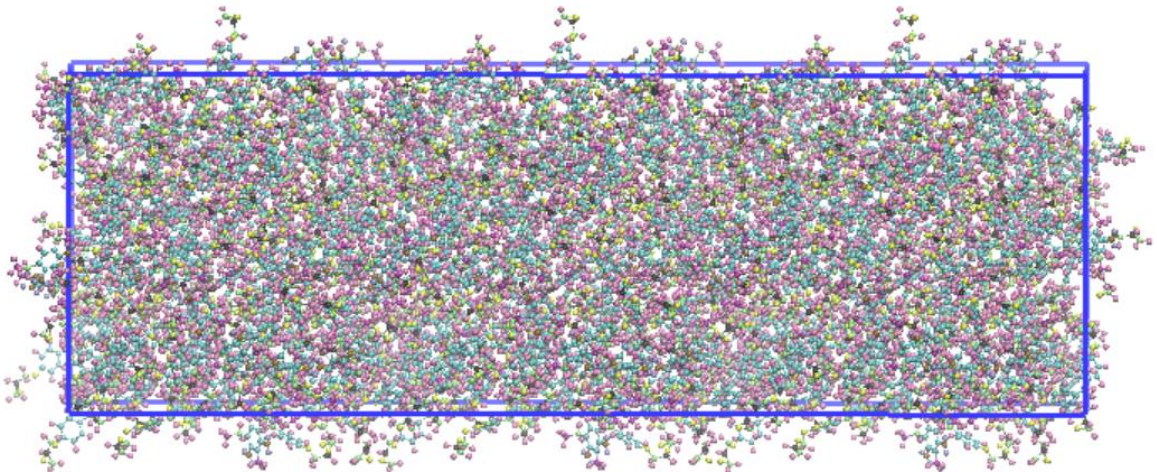

Fig. 6. Molecular model of epoxy for thermal conductivity evaluation.

3.1.2 Graphene

The graphene is 2D structure with a sheet of sp^2 carbon atoms. The graphene has been constructed by arranging carbon atoms in a hexagonal structure with a minimum distance of 1.42 Å and a bond angle of 120° between the atoms. Adaptive Intermolecular Reactive Empirical Bond Order (AIREBO) potential [50] available in LAMMPS software has been used to describe the bond interactions between the atoms. Thus, a graphene layer with a final size of 38.3 Å x 39.3 Å consisting of 576 atoms has been generated with periodic boundary conditions.

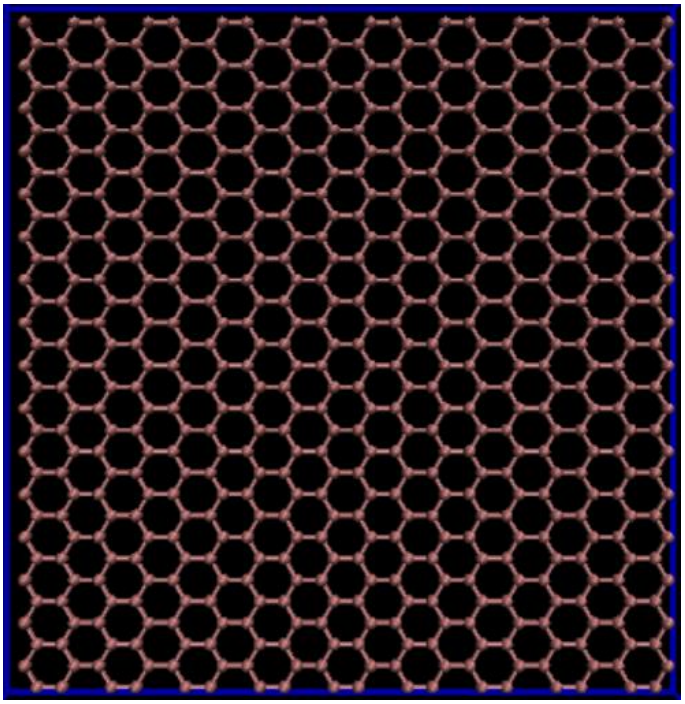

Fig. 7. Simulation model of graphene sheet.

3.1.3 Epoxy – Graphene Interface Model

To study the interfacial resistance at epoxy – graphene interface, a combined model of epoxy and graphene has been developed. The final structure of epoxy after equilibration mentioned in section 3.1.1 was used and replicated in z-direction to obtain a longer epoxy system. Further, the cross-section of epoxy is modified to match the size of graphene. A sandwich structure of size 38.3 Å x 39.3 Å x 200 Å has been constructed by inserting graphene sheet in between the epoxy. According to Luo and Lloyd [31], the study of size effect on interfacial thermal transport across polymer(paraffin)-graphene systems reveals that the interfacial thermal transport is immune to size effects when the length of polymer is more than 35 Å and width of cross-section is greater than 19.68 Å. The short mean free-path of atoms in polymer maybe the reason for this size-independence thus including all substantial vibrational modes within the size of 35 Å. The

interactions between epoxy and graphene atoms were defined as van der Waals (vdW) interactions using LJ potential parameters. The LJ potential parameters for carbon atoms in graphene were obtained from previously published work [32] and are mentioned in Table 1. The spacing between epoxy and the graphene sheet is approximately 3 Å. The combined structure of epoxy-graphene used for evaluation of interfacial thermal resistance is shown in Fig. 8. The combined structure is subject to equilibration in NVT and NPT ensembles before shifting it to NVE to obtain a temperature profile.

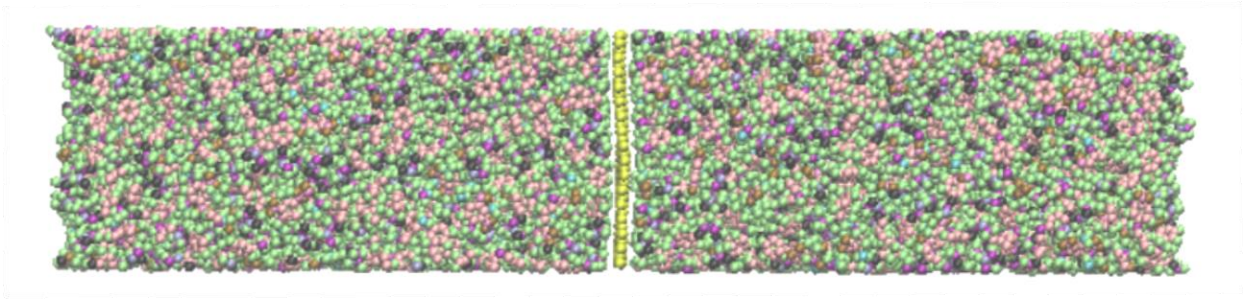

Fig. 8. Combined structure of epoxy-graphene.

3.2 Properties Predicted

The main objective of this research is to study the pressure dependence of thermal conductivity in epoxy and interfacial resistance at epoxy – graphene interface. The following properties have been evaluated for the same purpose.

1. Thermal Conductivity: Thermal conductivity of epoxy at different pressures determined by using NEMD method and calculated using Fourier's law.
2. Interfacial thermal resistance: Again, using NEMD method, interface resistance at epoxy-graphene interface is determined at different pressures to evaluate the pressure dependence.

The NEMD method and the equations used for calculation are discussed in the next section 3.3.

3.3 Methods

There are three methods known to measure the thermal conductivity [51, 27] of a material at an atomic level. The first one is the Equilibrium Molecular Dynamics method (EMD), mostly used to measure the bulk thermal conductivity of materials. This method makes use of the Green- Kubo relations for the calculation. The second method is the Non – Equilibrium Molecular Dynamics method (NEMD) [52], in which a temperature gradient is established in a system and is used to calculate thermal conductivity by Fourier law. The final method is a combination of determination of phonon dispersion relations and Landauer-Buttiker-type transport theory.

In this work, the classic Non-Equilibrium Molecular Dynamics (NEMD) method has been used to calculate the thermal conductivity in the epoxy and the interfacial thermal resistance at the epoxy-graphene interface.

The NEMD method is numerically a replica of the guarded heat plate experiment in which the sample is located between a hot source and cold source with thermostats at both the ends.

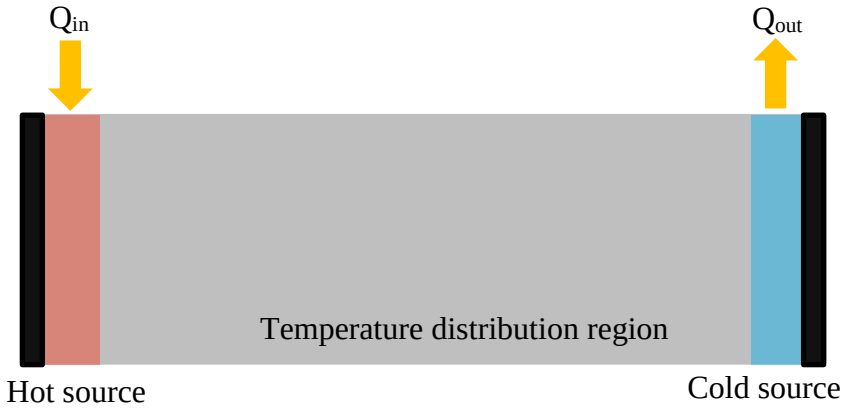

Fig. 9. Schematic of NEMD domain.

Thermal Conductivity by this method can be calculated in two ways; the first one is to apply a constant temperature gradient along the domain in z-direction and calculate the heat flux; while

the second method is to apply a constant flux and calculate the temperature gradient by obtaining a temperature distribution along the domain in z-direction. After a stable heat flow is obtained, the thermal conductivity would then be calculated by using temperature distribution as per the Fourier's law for heat flow,

$$J_q = -\kappa \nabla T \tag{3.3}$$

where J_q - the heat flux density,

κ - coefficient of thermal conductivity,

∇T - temperature gradient.

The second method of applying a constant heat flux has been employed in this case to measure the thermal conductivity of epoxy. To determine the temperature gradient, the simulation domain is divided into a number of slabs of same thickness. The temperature of the slab is calculated by

$$T_i = \frac{1}{3N_i k_B} \sum_{k}^{N_i} m_k {v_k}^2 \tag{3.4}$$

where T_i – instantaneous temperature for slab i,

N_i – number of atoms within slab i,

m_k – mass of atom k in slab i,

v_k – velocity of atom k in slab i,

k_B – Boltzmann constant

The temperature is then time-averaged to obtain a smooth curve. Once temperature distribution is obtained, and the slope of the curve is used as a temperature gradient to calculate the thermal conductivity.

To measure the interfacial resistance across graphene epoxy interface, the temperature at both ends has been fixed using Berendsen thermostats to establish a heat flow through the domain. The heat flux is generated in the system due to exchange of kinetic energy between atoms from hot and cold ends. Similar to the earlier case, the simulation domain has been divided into a number of slabs to calculate temperature and heat flux. The temperature of the slab is calculated as mentioned earlier and the following equation is used to calculate the heat flux in each slab.

$$J_q = \frac{\langle \frac{1}{2} \sum_{k=1}^{N_B} m_k (v_k'^2 - v_k^2) \rangle}{A \Delta T} \tag{3.5}$$

where A – area of the cross-section,

ΔT – the timestep of the simulation,

v_k, v_k' – atom velocities in hot and cold slab respectively.

The amount of heat flux in the system is obtained from LAMMPS. Once a stable temperature profile is established, the temperature difference at the interface is noted. The system is considered isometric and the temperature difference between graphene and epoxy at both sides of the interface is assumed to be equal.

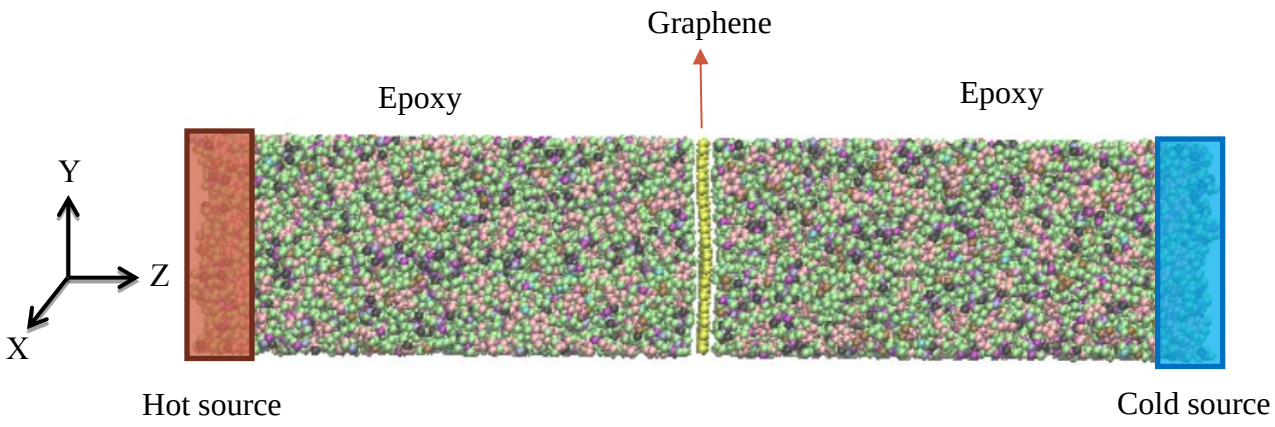

Fig. 10. NEMD domain for epoxy-graphene interface system.

The interfacial thermal resistance is calculated by

$$R_K = \Delta T / J_q \tag{3.6}$$

where R_K - interfacial thermal resistance,

J_q - the heat flux density,

ΔT - temperature difference between Graphene and Epoxy at the interface, which is equal to half of the temperature difference between the two epoxy surfaces.

3.4 Simulation/Run details

3.4.1 Epoxy System (Measurement of Thermal Conductivity)

As mentioned in section 3.1.1, after energy minimization, the system was subject to equilibration runs before shifting it to an NVE ensemble. To stabilize the temperature, the epoxy system was equilibrated in an NVT ensemble at 300 K for 200 ps. After a stable temperature is obtained, the system is then subject to NPT for 200 ps to obtain a stable pressure of 1 atm at 300 K. Then the simulation is shifted to an NVE ensemble where a certain amount of heat flux was supplied and removed to obtain a temperature distribution along the length of the domain. The simulation in NVE was allowed to run for 1000 ps to obtain a stable distribution.

For the pressure dependence studies, the system was subject to a different pressure in each case in the range of 0 – 10 GPa using an NPT ensemble and then shifted to NVE for temperature distribution measurement.

3.4.2 Epoxy – Graphene System (Measurement of Interfacial Thermal Resistance)

The epoxy-graphene interface model mentioned in section 3.1.3 is also subject to equilibration runs after energy minimization. The epoxy-graphene system was subject to an NVT simulation for 150 ps at 300 K followed by an NPT simulation at 1 atm, 300 K for 400 ps. The system is then

shifted to an NVE ensemble where the temperature at hot and cold ends has been fixed at 330 K and 270 K using Berendsen thermostats. The atoms at both the ends have been fixed by setting the velocity to zero. The simulation was allowed to run for 1500 ps to obtain a stable temperature distribution.

For pressure dependence studies, similar to the epoxy model, the system was subject to a different pressure in each case in the range of 0 – 10 GPa using an NPT ensemble and then shifted to NVE for temperature distribution measurement.

In both the cases, LJ cut off parameters were used for the short-range interactions and long-range correction has been applied for the coulombic interactions computed in k-space by using a PPPM technique.

3.4.3 Parameters in MD Simulations

A summary of all the parameters used in the MD simulations are mentioned in the tables below.

Table 2. Parameters used in simulations.

	Epoxy system (κ measurement)	**Epoxy-graphene (R_k measurement)**
Temperature	300 K	300 K
Pressure	0 – 10 GPa	0 – 10 GPa
NVE (temperature)	-	330 K – 270 K

Table 3. Methods and Controls used in LAMMPS.

	Epoxy system **(κ measurement)**	**Epoxy-graphene system** **(R_k measurement)**
Force-field	CVFF	CVFF and AIREBO potential
Temperature control	Nośe-Hoover	Berendsen
Pressure control	Nośe-Hoover	Nośe-Hoover
Short range simulation	van der Waals	van der Waals
Long range correction	PPPM	PPPM

4. RESULTS AND DISCUSSION

The model of epoxy generated and equilibrated as mentioned in the previous sections is subjected to MD in NVE ensemble to obtain a temperature distribution to estimate the thermal conductivity of epoxy. The value of thermal conductivity at 300 K and 1 atm pressure is evaluated and compared with the results from literature. Similar process was repeated for the evaluation of interfacial thermal resistance at epoxy – graphene interface 300 K and 1 atm and compared with the literature. This was done to validate the developed models and credibility of the results obtained from the simulations. Following this, the pressure dependence of the properties is studied by repeating the MD simulations at different pressures in range of 0 – 10 GPa. The results from the simulations and the evaluation of properties is explained in this chapter.

4.1 Thermal Conductivity of Epoxy

4.1.1 Thermal Conductivity Calculation

As a first step, the thermal conductivity of epoxy at 300 K, 1 atm was evaluated. The temperature distribution at steady-state is obtained from the NVE ensemble by adding and removing a fixed amount of heat from opposite ends of the system. The system is divided into number of slabs of equal size and the temperature of each slab is calculated for every 100000 samples stored at every 0.2 fs for 5000000 timesteps, i.e. 1000 ps. The temperature profile of the system is shown in Fig. 11.

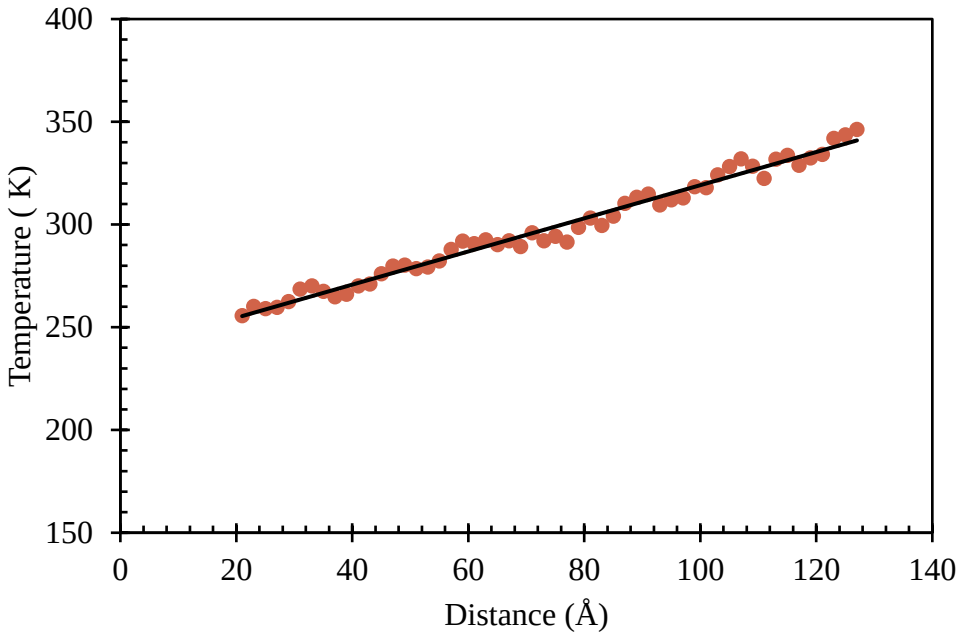

Fig. 11. Temperature profile along the length of the epoxy domain.

The slope of the curve between the hot and cold regions gives the temperature gradient in the system. By using Fourier's law stated in Equation (3.3) with the heat flux supplied and the obtained temperature gradient, the thermal conductivity of epoxy is calculated. The thermal conductivity of epoxy was calculated as 0.211 W m^{-1} K^{-1}. From the literature, the thermal conductivity of epoxy at room temperature by experimental measurements is approximately 0.25 W m^{-1} K^{-1} [4]. Varshney et al. [5] calculated the thermal conductivity of EPON – 862 and DEDTA by molecular dynamics and the values the in the range of 0.2 – 0.3 W m^{-1} K^{-1}. Therefore, the obtained thermal conductivity of epoxy matches well with the values by experimental and computational methods from the literature. Varshney et al. [5] also mention in their work that the size (number of slabs) of controlled regions (hot and cold regions) and the frequency at which the velocity is updated doesn't make a significant effect on the value of the thermal conductivity evaluated. The effect of these

parameters has been studied in published works [51] in which no significant variation in thermal conductivity has been observed.

Domain size effects are a very well-known characteristic in simulations. However, in this work, the size effect of simulation domain size has been neglected and a single domain size has been chosen for evaluation of thermal conductivity. Since the thermal conductivity of epoxy is very low, it is expected not to have a significant variation due to change in domain length. Also, one of the recent studies [29] in literature using EMD simulation shows that effect of domain size of epoxy is insignificant while evaluating thermal conductivity and thus substantiates the assumption.

4.1.2 Pressure Dependence of Thermal Conductivity

To study the pressure dependence of thermal conductivity, the epoxy model is subjected to different pressures in the range of 0 – 10 GPa in an NPT ensemble. The pressure applied was isometric and the system was allowed to compress in all directions. In the range of 0 – 1 GPa, a few different pressures have been studied at infrequent intervals, and in the range of 1 – 10 GPa, ten different pressures were tested at increments of 1 GPa. The change in volume of the system due to compression as a function of pressure is shown in the Fig. 12.

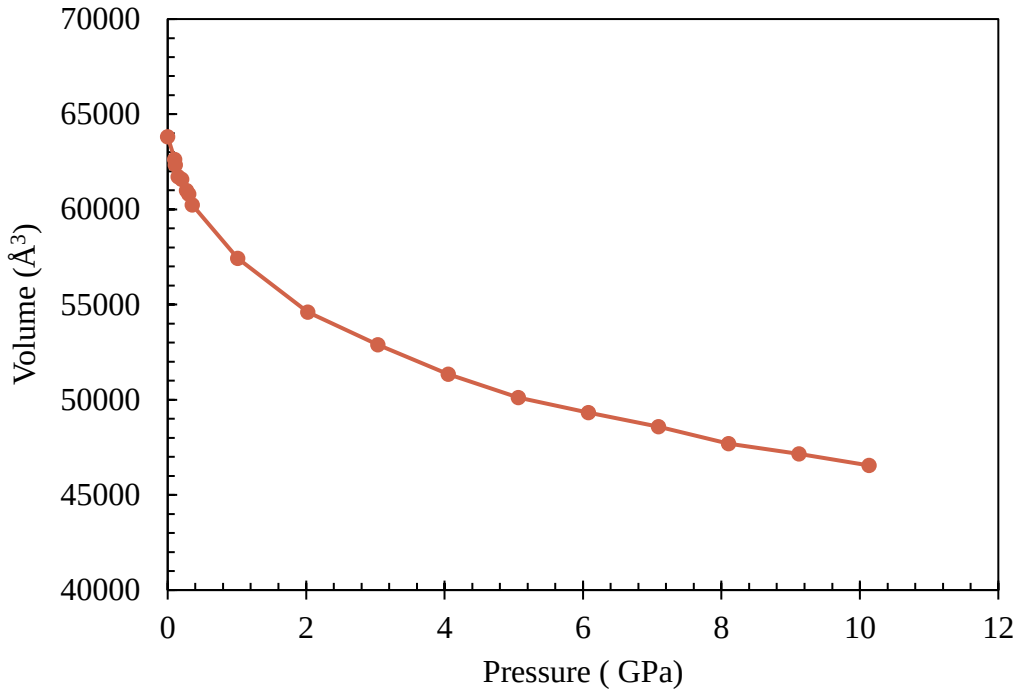

Fig. 12. Change in Volume of the epoxy system with pressure.

From the Fig. 12, it can be observed that the change in volume is steeper at lower pressures and the rate of change reduces as we move to higher pressures. This can be explained by the fact that the amount of free volume available in the system reduces as the pressure increases and therefore the rate of compression decreases as it becomes more difficult to compress the system. Free volume in polymers is the amount of unoccupied volume at the end of the polymer chain or around the chain molecules.

After the system is compressed at a particular pressure, it is then shifted to an NVE ensemble to obtain temperature gradient following the same method as mentioned above and the thermal conductivity is calculated by using the Fourier's law in Equation (3.3). The process is repeated for all the compressed volume models at different pressures. The pressure dependence of the evaluated

thermal conductivity of epoxy is shown in the Fig. 13Fig. 13. Variation of thermal conductivity with pressure (enlarged view of variation at low pressures in the box)

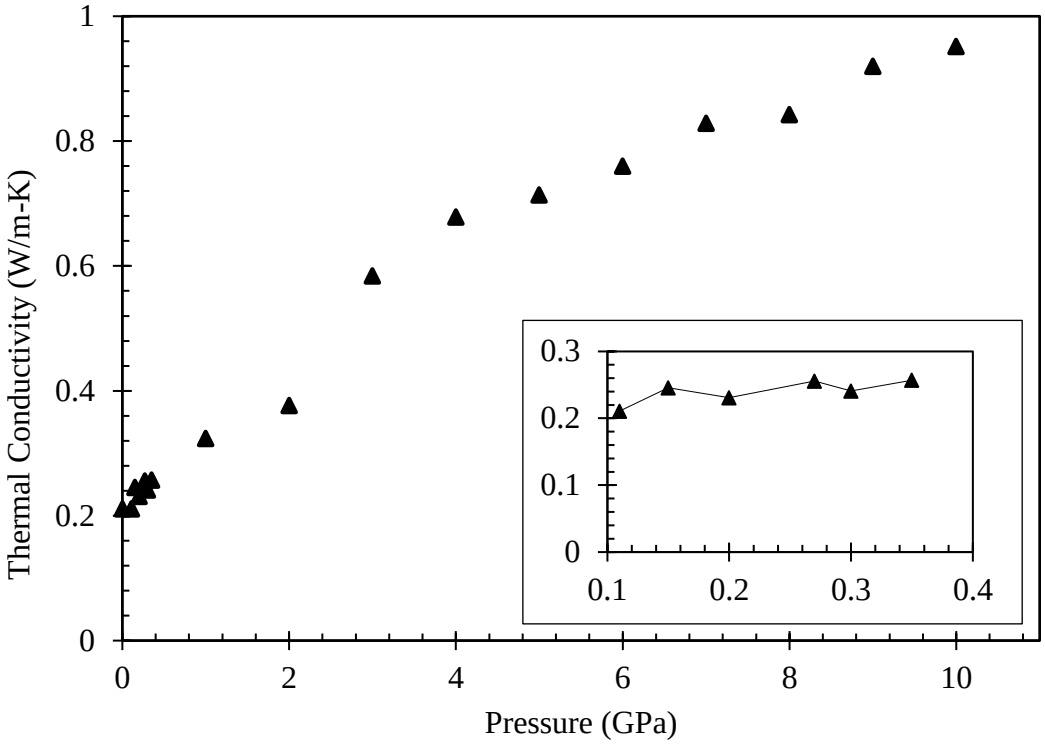

Fig. 13. Variation of thermal conductivity with pressure (enlarged view of variation at low pressures in the box).

From the Fig. 13, it can be observed that the thermal conductivity of epoxy increases with pressure. As the pressure increases, the volume of the system decreases thereby increasing the density and in turn, increases the thermal conductivity of the system. There are a very few studies [17, 18] in literature on the pressure dependence of thermal conductivity of epoxy, most of them being experimental and not very recent. These studies are limited to pressures up to a maximum of 2 GPa due to the practical limitations with the experimental setup. However, the evaluated thermal conductivity up to 2 GPa is in good agreement with the results from these experimental studies (about 0.38 W/m K at 2 GPa) [18] thus validating the thermal conductivity variation curve obtained

with respect to pressure. Therefore, the variation of thermal conductivity with respect to pressure shown in Fig. 13 can be used to predict values of thermal conductivity of epoxy at high pressures which is not currently available. However, it must be noted that there might be a certain amount of error/uncertainty in the values due to factors like precision in parallel simulations, accuracy of force-field at higher pressures.

4.1.3 Theoretical Prediction of Thermal Conductivity

In addition to the evaluation of thermal conductivity with respect to pressure from the MD simulations, the values of thermal conductivity at these pressures was predicted using the kinetic theory model for κ given by

$$\kappa = \frac{1}{3}\rho C_v s \Lambda \tag{4.1}$$

where ρ is the density, kg/m^3

C_v is the specific heat capacity at constant volume, J/kg-K

s is the average speed of sound, m/s.

The average speed of sound can be calculated from Bulk modulus and density using the following relation,

$$s = \sqrt{\frac{B}{\rho}} \tag{4.2}$$

where B is the Bulk Modulus (pressure dependent), Pa

Λ is the length of the phonon mean free path given by,

$$\Lambda = \frac{1}{\pi d^2 n_v} \tag{4.3}$$

where d is the diameter of the spherical molecule, and n_v is defined by the relation below,

$$n_v = \frac{Number\ of\ molecules}{Unit\ volume} = \frac{P}{k_B T} \tag{4.4}$$

To predict the value of thermal conductivity for the points in the pressure range, all the above-mentioned quantities were evaluated using the equations.

For the calculation of average speed of sound, s, the density was obtained directly as an output from the MD simulations. Bulk Modulus, the resistance to compression exhibited by the material is given by a ratio of change in pressure to the strain in the system and also called as the incompressibility.

$$B = -V\frac{dP}{dV} \tag{4.5}$$

where B is the bulk modulus,

V - initial volume of the system,

dP - change in pressure,

dV - change in volume due to pressure.

The bulk modulus, B, at different pressures was calculated using the change in volume upon compression data from Fig. 12. The variation of bulk modulus with respect to pressure is shown in the Fig. 14.

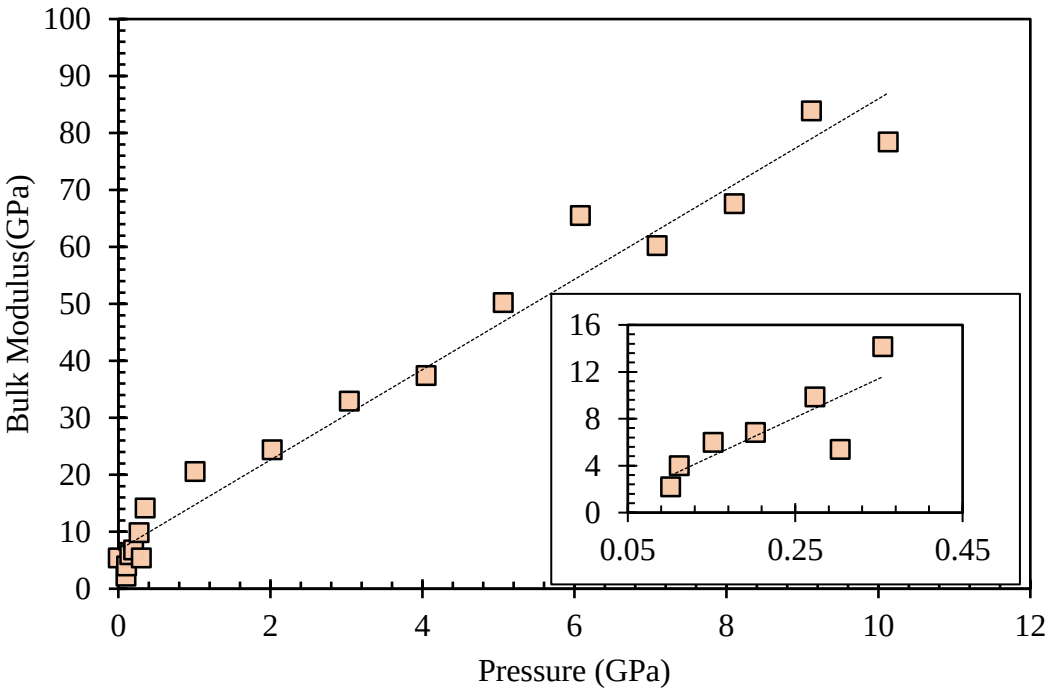

Fig. 14. Bulk Modulus of epoxy with respect to pressure (enlarged view of low-pressure variation in the box).

The bulk modulus was calculated by applying a finite difference approach, central difference scheme at every pressure. However, in the region of lower pressures, because the simulations were performed at pressures at slightly irregular intervals and for the first and last values, a forward diferrence or backward difference method has been used as per suitability. This might result in a slight error(irregularity) in the values of the bulk modulus, but not in the main range of interest of 1 – 9 GPa. The average speed of sound, s, was obtained using the bulk modulus data from Fig. 14 and the density from the simulation results.

The specific heat capacity for epoxy was taken as 1060 J kg^{-1} K^{-1} with reference to published works [53, 30] from literature. It is difficult to calculate the phonon mean free path from the Equation (4.3) due to ambiguity related to d, diameter of the spherical molecule which is not applicable in

case of epoxy with molecule chains. The mean free path must be estimated by other means such as based on dilatational wave velocity [30]. Therefore, a value for phonon mean free path of epoxy was used from literature. The phonon mean free path is estimated to be in the range of (0.11 – 0.3 nm) by several researchers [54, 30]. In the current work, the phonon mean free path of epoxy was considered as 0.25 nm. The choice is validated by the value of predicted thermal conductivity at 1 atm pressure, 0.218 W m^{-1} K, which matches the value from the simulation. The predicted thermal conductivity of epoxy using the kinetic theory model and a comparison of predicted and simulation values in shown in the Fig. 15 below.

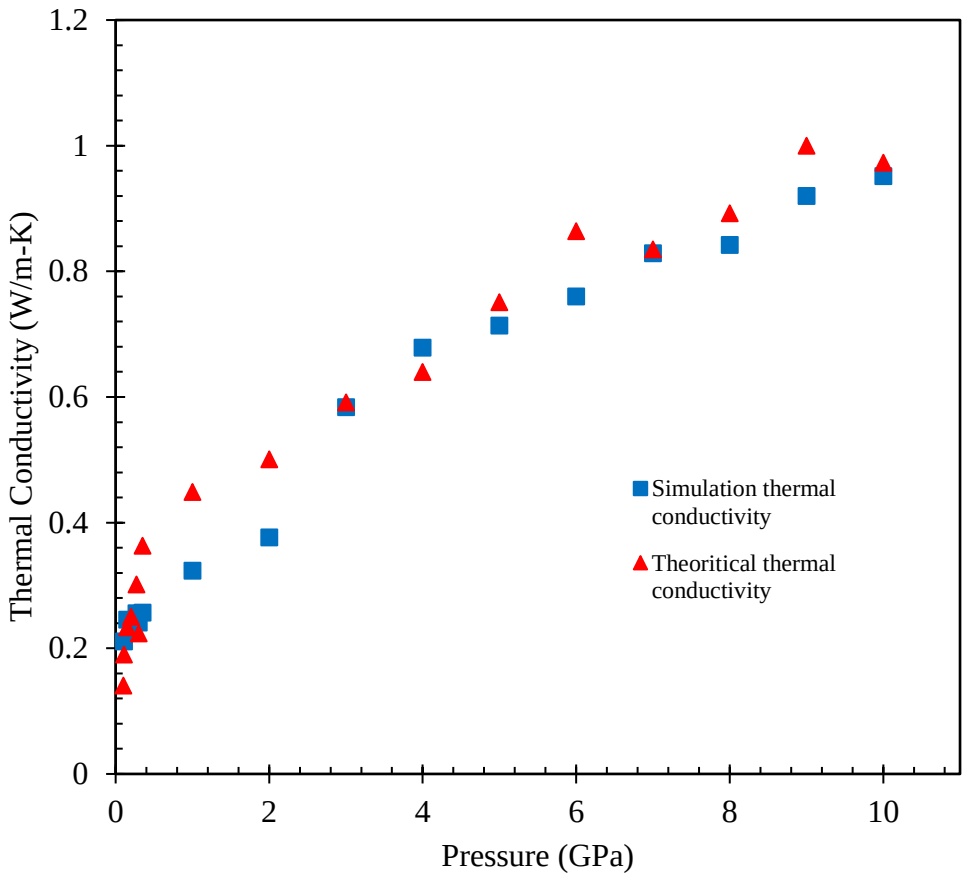

Fig. 15. Comparison of predicted and simulation thermal conductivities.

From the Fig. 15, it is seen that the theoretical (using kinetic theory) and evaluated (from simulation) are in agreement with each other. The results from the theoretical model show that the density and the average speed of sound are the factors that significantly influence the change in thermal conductivity with pressure. However, it is clearly noticeable that they follow a similar trend of pressure dependence and match each other to a reasonable extent.

4.2 Interfacial Thermal Resistance at Epoxy – Graphene Interface

4.2.1 Calculation of Interfacial Thermal Resistance

Similar to the evaluation of thermal conductivity, an NEMD method was used to calculate the interfacial thermal resistance. However, a slightly different approach was used to generate heat flux in the system. The entire domain is divided into number of slabs and two slabs on the either ends of the domain are defined as the hot and cold regions. The hot region was fixed at 340 K and the cold region was kept at 260 K using Berendsen thermostats. Heat flux in generated in the system by exchange of kinetic energy of atoms from the hot and cold regions. Fig. 16 gives the variation of cumulative heat flux (input from hot region and removed from cold region) with respect to time.

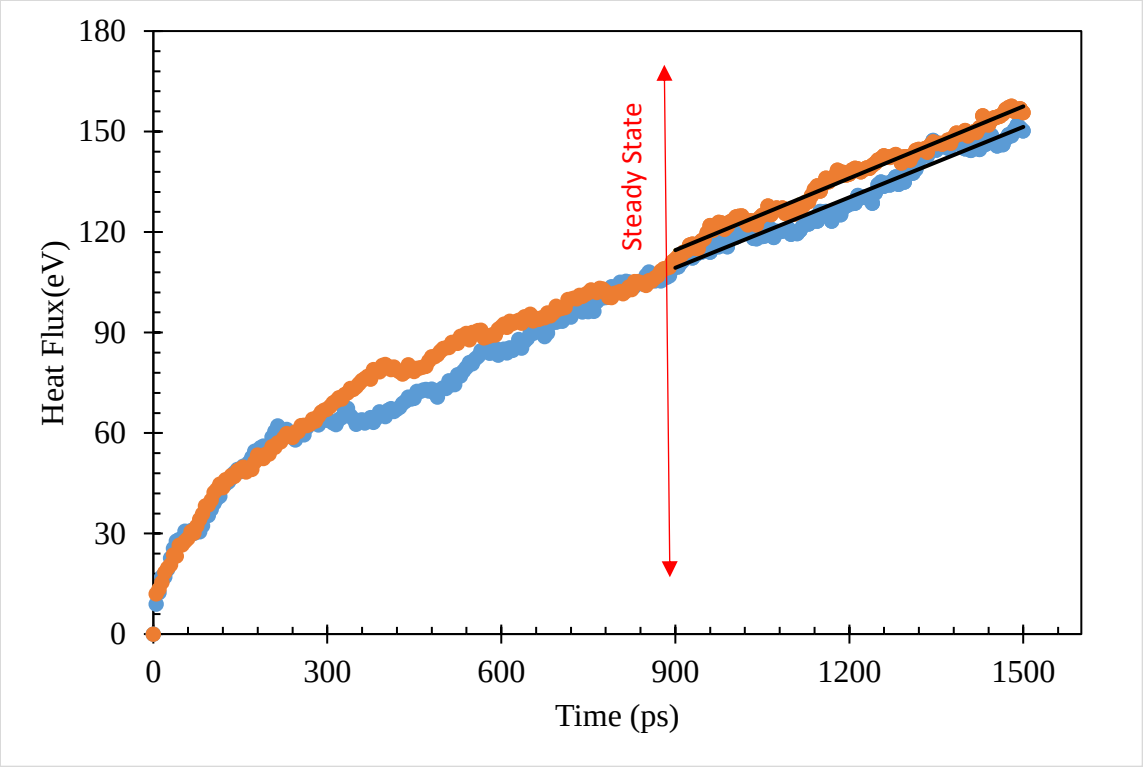

Fig. 16. Heat flux variation with time, series 1(orange) - energy input into the system, series 2 (blue) - energy removed from the system.

On reaching the steady state, the slope for both the curves should be equal and parallel. It can be seen from the Fig. 16 that the slope for both the curves is parallel after approximately 900 ps. Thus, it can be said that the steady state of the system is reached after 900 ps after which the heat flux per unit time can be calculated. Once the steady state is reached the heat flux per unit time was obtained from the slope of the curve.

Similar to the earlier case, the temperature distribution in the system with distance (across the slabs in z – direction) due to the generated heat flux at steady state was obtained from the simulation. The temperature of each slab was calculated for every 0.0005 ps for 1500 ps. The Fig. 17 shows the variation of temperature along the domain of epoxy-graphene in z – direction.

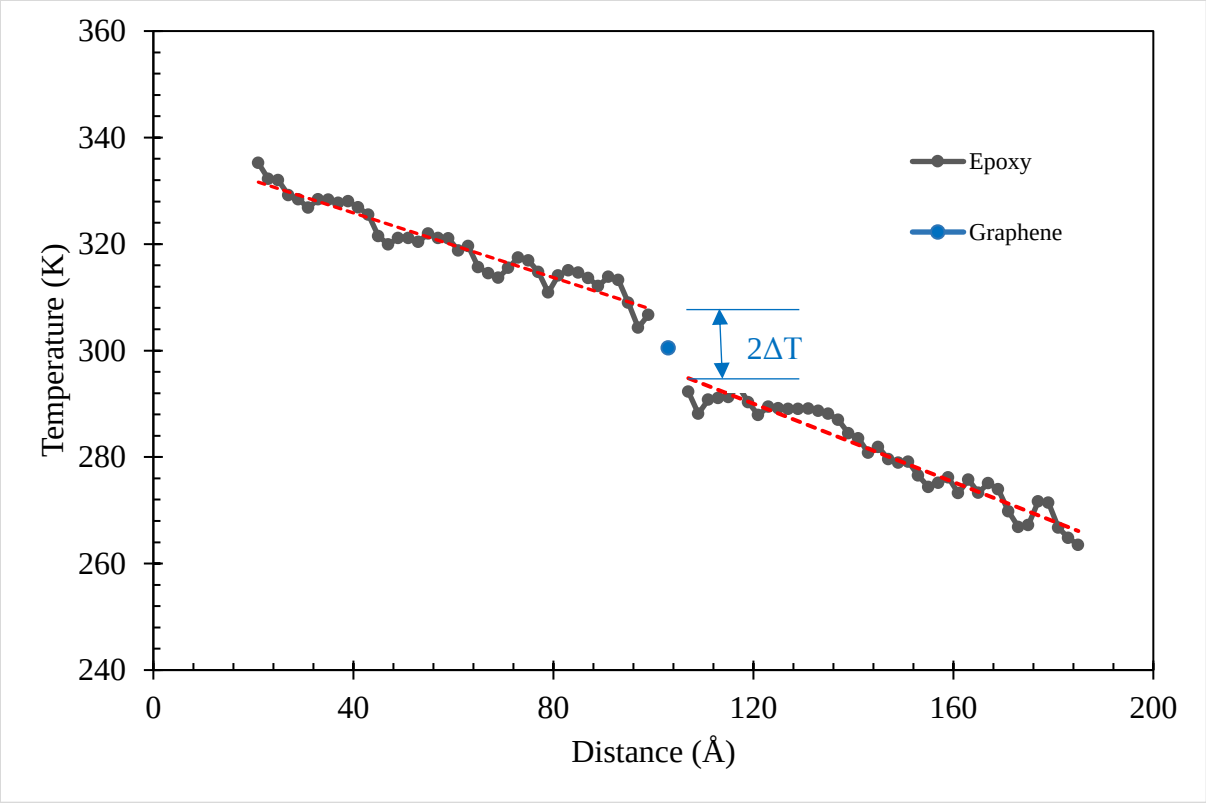

Fig. 17. Temperature profile in epoxy-graphene interface model.

From the Fig. 17, it can be observed that there is a significant temperature difference between the epoxy and graphene surfaces. The corresponding interfacial thermal resistance at the epoxy – graphene was calculated using the Equation (3.4). The value of interfacial thermal resistance was obtained as 0.776×10^{-8} m^2 KW^{-1}. This value is in good agreement with $(0.713 \pm 0.036) \times 10^{-8}$ m^2 KW^{-1} [32] reported in the literature.

Thermal conductivity for the epoxy part of the domain has also been computed from the obtained temperature distribution for the purpose of verification. The thermal conductivity of epoxy in the epoxy – graphene interface model was obtained as 0.22 W m^{-1} K^{-1} which is close to the value calculated from the pure epoxy system which is 0.211 W m^{-1} K^{-1}.

There are two important factors to be noted in the present work. In this work, the focus was only on single-layer graphene. The effect of stacking more layers of graphene was not considered or studied though the applications of graphene in nanocomposite matrix could be of single or multi layers. This is because, previous MD studies [55, 2] on interfacial resistance at polymer-graphene interfaces have demonstrated that there is no significant effect of number of layers of graphene on the interfacial resistance up to 5 layers.

Secondly, only a single size domain has been tested for interfacial thermal resistance due to the reasons mentioned earlier in 3.3 stating that the size effects in polymer are negligible when the domain length is greater than 35 Å and cross-section greater than 19.68 Å. However, studies [33] show that the length of the graphene might have an effect on its thermal conductivity which has not been studied in this work.

4.2.2 Pressure Dependence of Interfacial Thermal Resistance

To study the pressure dependence of interfacial, the epoxy-graphene model is subjected to different pressures in the range of 0 – 10 GPa in an NPT ensemble. The pressure applied was applied in the axial direction. The system was allowed to compress only in the axial direction so that the epoxy – graphene interface cross-section is unaffected and any undesired behavior of graphene such as bending of graphene sheet due to pressure in in-plane direction may be avoided. In the range of 0 – 1 GPa, a few different pressures have been studied at infrequent intervals, and in the range of 1 – 10 GPa, ten different pressures were tested at increments of 1 GPa.

After the system is compressed at a particular pressure, it is then shifted to an NVE ensemble to obtain temperature gradient following the same method as mentioned above and the interfacial

thermal resistance is calculated by using Equation (3.4). The process is repeated for all the compressed volume models at different pressures. The pressure dependence of the obtained interfacial thermal resistance is shown in the Fig. 18.

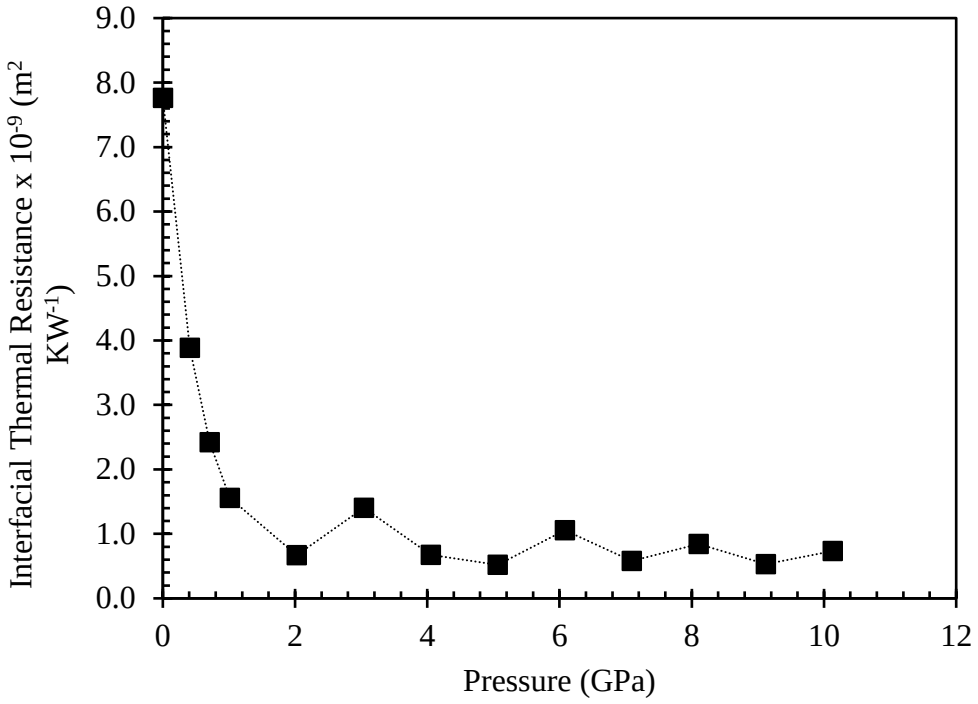

Fig. 18. Variation of Interfacial thermal resistance with respect to pressure in epoxy-graphene model. The dash line is to guide the eyes.

From the Fig. 18, it can be observed that the interfacial thermal resistance has a strong dependence on pressure. Some researchers have explained that a weak dependence of interfacial resistance on pressure is observed at strong bonding interfaces and vice versa. Hence, the strong dependence in this case can be explained by the same fact since the interface between epoxy and graphene surfaces does not comprise of strong chemical/physical bonds [21]. In Fig. 18, a rapid decrease in interfacial thermal resistance is observed in the lower pressure range and eventually the rate of

decrease is lower as it reaches saturation. Nearly 80% percent improvement in interfacial resistance is observed at 1 GPa at which the compressive strain is around 20%.

There are no studies available in the literature that discuss the pressure dependence in polymer – graphene interfaces. However, there are a few available studies on pressure dependence of interface resistance at other graphene interfaces. From one such published work, it is observed that at graphene – MoS_2 interface, a 150% improvement in ITR was observed at 5% compressive strain loading [36]. The variation is similar to the observed in the current study, though the rate of variation is comparatively higher in case of graphene – MoS_2 interface which may be attributed to the fact that MoS_2 possesses a higher thermal conductivity than epoxy in the first place and a system of graphene - MoS_2 may be experiencing a higher phonon transport as well overcoming the resistance faster. The decrease in ITR with increase in pressure can be explained by a phenomenon studied by Hseih et al. [56] As the pressure applied on the system increases, the stiffness of the interface would increase, especially at weakly bonded interfaces. Few other studies have shown that the ITR is strongly dependent on the interfacial stiffness. Therefore, the variation of ITR in the current study can be explained by an increase in interfacial stiffness with pressure which causes an increase in the phonon transmission and hence result in a lower interfacial thermal resistance.

Also, few other studies have suggested that the Debye frequency in a system increases with increase in pressure. An increased Debye frequency would result in increased limit for Phonon Density of States (PDOS) thus enabling added inelastic phonon channels thereby resulting in increased phonon transmission and lower interfacial thermal resistance.

Overall, it can be concluded that interfacial thermal resistance in epoxy – graphene is strongly dependent on pressure. A pressure under 10 GPa can reduce the interfacial thermal resistance in these systems almost close to 100%. This is very useful property that can be explored to achieve desirable heat transport characteristics in nanocomposite systems.

5. CONCLUSIONS

5.1 Summary

Overall, this study of epoxy and epoxy-graphene system using non-equilibrium molecular dynamics (NEMD) simulations focuses on two important thermal properties, thermal conductivity of epoxy and the interfacial thermal resistance at epoxy-graphene interface and their pressure dependent behavior. LAMMPS, an open source software by Sandia national laboratory was used to perform the MD simulations.

The models of epoxy and epoxy graphene system were developed using LAMMPS. The interactions between epoxy atoms were defined using a Consistent Valence Forcefield (CVFF) forcefield and the interactions between carbon atoms in graphene were described by the Adaptive Intermolecular Reactive Empirical Bond Order (AIREBO) potential. Van der Waals (vdW) interactions using LJ potential parameters were described for the interactions of epoxy with graphene atoms and non-bonded interactions within epoxy atoms. Long range correction was implemented for the long-range coulombic interactions using the PPPM technique. The process and the parameters of the simulation including the minimization and the equilibration stages has been discussed in detail.

From the results of the simulation, first of all, the thermal conductivity of epoxy was evaluated to be 0.211 W m^{-1} K^{-1} at 300 K and 1 atm pressure. Next, the epoxy was subjected to isometric compression at several pressures in the range of 1 - 10 GPa. The thermal conductivity for epoxy was estimated at all the pressures in the range to obtain a pressure dependence of the thermal

conductivity. Theoretical prediction of thermal conductivity was also done using the kinetic theory model for thermal conductivity and the results were compared to the simulation results which are in good agreement with each other. In the process of theoretical prediction, bulk modulus of epoxy was also evaluated at different pressures between 1 - 10 GPa.

Further, using the epoxy-graphene interface model, the interfacial thermal resistance at the epoxy-graphene interface was predicted to be approximately 0.776×10^{-8} m^2 KW^{-1}, which matches well with the literature. Similar to the case of thermal conductivity, the system was subject to different pressures in the range of 1 – 10 GPa and the pressure dependence of interfacial thermal resistance at epoxy-graphene interfaces was studied. It is observed that interfacial thermal resistance significantly decreases with increase in pressure. At a compressive pressure of 10 GPa, nearly 90-95 % improvement in interfacial thermal resistance was observed.

The pressure dependence of thermal conductivity and interfacial thermal resistance; their improvement with increase in pressure can be beneficial if used suitably to improve the efficiency of TIMs and heat dissipation in the devices using them.

5.2 Future Scope of Work

It is understood from few studies in literature, that tensile and compressive strain affect the interfacial thermal resistance. Though, it is known that a tensile pressure increases the interfacial resistance and a compressive pressure decreases it, the rate of increase and decrease seem to be different for same percentage of strain applied. Therefore, the behavior of these properties under both tensile and compressive situations may be studied to get a better understanding of the pressure dependent behavior and be used in applications appropriately.

A helpful idea to improve performance of epoxy-graphene systems might be to align the epoxy chains in a systematic manner which would improve the thermal conductivity due to superior phonon transport and then apply a compressive pressure to further augment the efficiency by reducing the interfacial thermal resistance.

Finally, though it is well researched and established that size effects in polymer are insignificant in the study of thermal conductivity and interfacial thermal transport, the size of graphene is still expected to be important. It is discussed in literature that increasing the cross-section of graphene significantly may reduce the interfacial thermal resistance due to the longer mean free path of phonons in graphene. Further research may be conducted on these terms to study the pressure dependent behavior with size effects of graphene in consideration.

REFERENCES

[1] J. Schleeh, J. Mateos, I. Íiguez-de-la-Torre, N. Wadefalk, P. A. Nilsson, J. Grahn and A. J. Minnich, "Phonon black-body radiation limit for heat dissipation in electronics," *Nature Materials,* vol. 14, no. 2, pp. 187-192, 2015.

[2] Y. Wang, H. F. Zhang, Y. Xiang, C. Yang, C. Wang and Y. Zhang, "Effect of covalent functionalization on thermal transport across graphene-polymer interfaces," *The journal of physical chemistry C,* vol. 119, no. 22, pp. 12731 - 12738, 2015.

[3] R. Prasher, J. Y. Chang, I. Sauciuc, S. Narasimhan, D. Chau, G. Chrysler, A. Myers, S. Prstic and C. Hu, "Nano and Micro Technology-Based Next-Generation Package-Level Cooling Solutions," *Intel Technology Journal,* vol. 9, pp. 285 - 296, 2005.

[4] D. E. Kline, "Thermal Conductivity of Polymers," *Journal of Polymer Science,* vol. 50, no. 154, pp. 441-450, 1961.

[5] V. Varshney, S. Patnaik, A. Roy and B. Farmer, "Heat Transport in Epoxy Networks: A molecular dynamics study," *Polymer,* vol. 50, pp. 3378-3385, 2009.

[6] H. Chen, V. V. Ginzburg, J. Yang, Y. Yang and W. Liu, "Thermal conductivity of polymer-based composites:," *Progress in Polymer Science,* vol. 59, pp. 41-85, 2016.

[7] J. Liu, T. Wang, B. Carlberg and M. Inoue, "Recent progress of thermal interface materials," in *2nd Electronics System-Integration Technology Conference,* 2008.

[8] F. Sarvar, D. C. Whalley and P. P. Conway, "Thermal Interface Materials - A Review of the State of the Art," in *1st IEEE Electronic Systemintegration Technology Conference* , Dresden, 2006.

[9] A. Kausar, I. Rafique and B. Muhammad, "Review of Applications of Polymer/Carbon Nanotubes and Epoxy/CNT Composites," *Polymer-Plastics Technology and Engineering* , vol. 57, no. 11, pp. 1167-1191, 2016.

[10] N. Luhyna and F. Inam, "Carbon Nanotubes for Epoxy Nanocomposites: A Review on Recent Developments," in *2nd International Conference on Advanced Composite Materials and Technologies for Aerospace Applications*, Wrexham, 2012.

[11] M. Yoonessi, M. Lebrón-Colón, D. Scheiman and M. A. Meador, "Carbon Nanotube Epoxy Nanocomposites: The Effects of Interfacial Modifications on the Dynamic Mechanical Properties of the Nanocomposites," *ACS Applied Materials & Interfaces*, vol. 6, no. 19, pp. 6621-6630, 2014.

[12] E. H. Backes, T. S. Sene, F. R. Passador and L. A. Pessan, "Electrical, Thermal and Mechanical Properties of Epoxy/CNT/Calcium Carbonate," *Materials Research,* vol. 21, no. 1, 2018.

[13] S. Stankovich, D. A. Dikin, G. H. B. Dommett, K. M. Kohlhaas, E. J. Zimney, E. A. Stach, R. D. Piner, S. T. Nguyen and R. S. Ruoff, "Graphene-based composite materials," *Nature*, vol. 442, pp. 282-286, 2006.

[14] S. Ghosh, I. Calizo, D. Teweldebrhan, E. P. Pokatilov, D. L. Nika, A. A. Balandin, W. Bao, F. Miao and C. N. Lau, "Extremely high thermal conductivity of graphene: Prospects for thermal management applications in nanoelectronic circuits," *Applied Physics Letters,* vol. 92, no. 15, 2008.

[15] A. A. Balandin, S. Ghosh, W. Bao, I. Calizo, D. Teweldebrhan, F. Miao and C. N. Lau, "Superior Thermal Conductivity of Single-Layer Graphene," *Nano Letters,* vol. 8, no. 3, pp. 902-907, 2008.

[16] G. L. Pollack, "Kapitza resistance," *Review of Modern Pysics,* vol. 41, no. 1, pp. 48-81, 1969.

[17] P. Andersson and G. Bäckström, "Pressure dependence of the thermal conductivity of an epoxy resin," *Journal of Applied Physics,* vol. 44, no. 2, pp. 705 - 707, 1973.

[18] B. Sundqvist, O. Sandberg and G. Backstrom, "The thermal properties of an epoxy resin at high pressure and temperature," *Jounal of Physics D: Applied Physics,* vol. 10, pp. 1397 - 1403, 1977.

[19] A. Pham, M. Barisik and B. Kim, "Pressure dependence of Kapitza resistance at gold/water and silicon/water interfaces," *The Journal of chemical physics,* vol. 139, p. 244702, 2013.

[20] R. Peterson and A. Anderson, "Acoustic-mismatch model of the Kapitza resistance," *Physics Letters A,* vol. 40, no. 4, pp. 317-319, 1972.

[21] P. Zhang, P. Yang, X. Jiang, S. Zhai, Y. Xian, H. Qin and D. Yang, "A theoretical review on interfacial thermal transport at the nanoscale," *Small,* vol. 14, no. 2, p. 1702769, 2018.

[22] C. Liu, Z. Wei, W. Chen, K. Bi, J. Yang and Y. Chen, "Pressure effects on the thermal resistance of few-layer graphene," *Physics Letters A,* vol. 380, pp. 248-254, 2015.

[23] E. Swartz and R. O. Pohl, "Thermal boundary resistance," *Reviw of Modern Physics,* vol. 61, no. 3, pp. 605-668, 1989.

[24] P. Debye, "The early days of lattice dynamics," in *Lattice Dynamics*, Pergamon, 1965, pp. 9-13.

[25] M. Dove, "Introduction to the theory of lattice dynamics," *Collection SFN,* vol. 12, pp. 123-129, 2011.

[26] W. G. Hoover, "Molecular Dynamics," *Lecture Notes in Pysics,* vol. 258, 1986.

[27] D. Frenkel and B. Smit, Understanding Molecular Simulation: From Algorithms to Applications, Academic Press, 1996.

[28] A. Kumar, V. Sundararaghavan and A. Browning, "Study of temperature dependence of thermal conductivity in cross-linked epoxies using molecular dynamics simulations with long range interactions," *Modelling and Simulation in Materials Science and ENgineering,* vol. 22, p. 15, 2014.

[29] S. Li, X. Yu, H. Bao and N. Yang, "High thermal conductivity of bulk epoxy resin by bottom-up parallel linking and strain: a molecular dynamics study," *The Journal of Physical Chemistry C,* vol. 122, no. 24, pp. 13140-13147, 2018.

[30] P. B. Kaul, M. F. Bifano and V. Prakash, "Multifunctional carbon nanotube-epoxy composites for thermal energy management," *Journal of Composite Materials,* vol. 47, no. 1, pp. 77 - 95, 2013.

[31] T. Luo and J. R. Lloyd, "Enhancement of Thermal Energy Transport Across Graphene/Graphite and Polymer Interfaces: A Molecular Dynamics Study," *Advanced Functional Materials,* vol. 22, no. 12, pp. 2495-2502, 2012.

[32] Y. Wang, C. Yang, Q. X. Pei and Y. Zhang, "Some Aspects of Thermal Transport across the Interface between Graphene and Epoxy in Nanocomposites," *ACS Applied Materials & Interfaces,* vol. 8, no. 12, pp. 8272-8279, 2016.

[33] M. Wang, D. Galpaya, Z. B. Lai, Y. Xu and C. Yan, "Surface functionalization on thermal conductivity of graphene-polymer nanocomposites," *Internal Journal of Smart and Nano Materials,* vol. 5, no. 2, pp. 123-132, 2014.

[34] G. T. Hohensee, M. R. Fellinger, D. R. Trinkle and D. G. Cahill, "Thermal transport across high-pressure semiconductor-metal transition in Si and Si0.991 Ge0.009," *Physical Review B,* vol. 91, 2015.

[35] B. Liu, J. A. Baimova, C. D. Reddy, S. V. Dmitriev, W. K. Law, X. Q. Feng and K. Zhou, "Interface thermal conductance and rectification in hybrid graphene/silicene monolayer," *Carbon,* vol. 79, pp. 236-244, 2014.

[36] Z. Ding, Q. X. Pei, J. W. Jiang and W. Huang, "Interfacial thermal conductance in graphene/MoS2 heterostructures," *Carbon,* vol. 96, pp. 888 - 896, 2015.

[37] A. Hospital, J. Goni, M. Orozco and J. Gelpi, " Molecular dynamics simulations: advances and applications," *Adv Appl Bioinform Chem.,* pp. 37-47, 2015.

[38] S. Plimpton, P. Crozier and A. Thompson, "LAMMPS Documentation," 2006.

[39] M. Allen, "Introduction to Molecular Dynamics Simulation," *Computational Soft Matter: From Synthetic Polymers to Proteins,* vol. 23, pp. 1-28, 2004.

[40] S. Toxvaerd and J. C. Dyrea, "Communication: Shifted forces in molecular dynamics," *The Journal of Chemical Physics,* vol. 134, 2011.

[41] L. Verlet, "Computer "Experiments" on Classical Fluids. I. Thermodynamical Properties of Lennard-Jones Molecules," *Physical Review,* vol. 159, no. 1, pp. 98-103, 1967.

[42] R. Hockney, "Potential Calculation and Some Applications," *Methods in Computational Physics,* vol. 9, pp. 135-211, 1970.

[43] W. C. Swope, H. C. Andersen, P. H. Berens and K. R. Wilson, "The velocity verlet algorithm," *The Journal of Chemical Physics,* vol. 76, pp. 637-649, 1982.

[44] M. R. Hestenes and E. Stiefel, "Methods of Conjugate Gradients for Solving Linear Systems," *Journal of Research of the National Bureau of Standards,* vol. 49, no. 6, pp. 409-436, 1952.

[45] A. Bandyopadhyay and G. M. Odegard, "Molecular modelling of physical aging in epoxy polymers," *Journal of Applied Polymer Science,* vol. 128, no. 1, pp. 660-666, 2012.

[46] H. Lorentz, *Ann. Phys.,* vol. 248, pp. 127-136, 1881.

[47] D. Berthelot, *Compt. Rendus,* vol. 126, pp. 1703-1706, 1898.

[48] S. Plimpton, "Fast Parallel Algorithms for Short-Range Molecular Dynamics," *Journal of Compuational Physics,* vol. 117, pp. 1-19, 1995.

[49] A. Bandopadhyay, P. K. Valavala, T. C. Clancy, K. E. Wise and G. Odegard, "Molecular modeling of crosslinked epoxy polymers: The effect of crosslink density on thermomechanical properties," *Polymer,* vol. 52, no. 11, pp. 2445-2452, 2011.

[50] S. J. Stuart, A. B. Tutein and J. A. Harrison, "A reactive potential for hydrocarbons with intermolecular interactions," *Journal of Chemical Physics,* vol. 112, no. 14, pp. 6472-6486, 2000.

[51] P. Chantrenne and J. L. Barrat, "Finite Size Effects in Determination of Thermal Conductivities: Comparing Molecular Dynamics Results with Simple Models," *J. Heat Transfer,* vol. 126, no. 4, pp. 577-585, 2004.

[52] F. Muller-Plathe, "A simple nonequilibrium molecular dynamics method for calculating the thermal conductivity," *The Journal of Chemical Physics*, vol. 106, no. 14, pp. 6082-6085, 1997.

[53] C. Li, G. A. Mendvedev, E. W. Lee, J. Kim, J. M. Caruthers and A. Strachan, "Molecular dynamics simulations and experimental studies of the thermomechanical response of an epoxy thermoset polymer," *Polymer,* vol. 53, no. 19, pp. 4222-4230, 2012.

[54] G. Chen, "Thermal conductivity and ballistic-phonon transport in the cross-plane direction of superlattices," *Physical Review B,* vol. 57, no. 23, pp. 14958-14973, 1998.

[55] L. Hu, T. Desai and P. Keblinski, "Determination of interfacial thermal resistance at nanoscale," *Physical Review B,* vol. 83, no. 5, p. 195423, 2011.

[56] W. P. Hseih, A. S. Lyons, E. Pop, P. Keblinski and D. G. Cahill, "Pressure tuning of the thermal conductance at weak interfaces," *Physical Review B,* vol. 84, no. 8, p. 184107, 2011.

[57] M. Steinhauser, "Introduction to Molecular Dynamics Simulations: Applications in Hard and Soft Condensed Matter Physics," 2012.